Università degli Studi di Padova

Dipartimento di Beni Culturali: Archaeologia, Storia dell' Arte, del Cinema e della Musica

Corso di Laurea Magistrale in

SCIENZE ARCHEOLOGICHE

Curriculum in

APPLIED SCIENCES TO CULTURAL HERITAGE MATERIALS AND SITES

Double Master degree with the

University of Haifa

Master Mention

Maritime Civilizations

Hydraulic properties of the mortars at Miriam's Well beach, Tiberias (Israel)

Co-supervisors:

Prof. Emmanuel Nantet

Prof. Michele Secco

Candidate: Konstantinos Thomas

Matricola: 2039387

Academic year 2022-2023

Aknwoledgements

I would like to express my appreciation to my supervisor professor Emmanuel Nantet of the University of Haifa for his assisatnce regarding the selection of the research topic and his precious support during the wiriting of my thesis.

Also I am thankful to my second supervisor professor Michele Secco for his assistance and his valuable advice during the chemical and mineralogical analyses which took place at the facilities of the University of Padova.

Moreover, I am grateful to my professor Ruth Shahak-Gross for her help during the FTIR analyses at the facilities of her lab at the University of Haifa.

Furthermore, I would like to express my gratidute to Dr Andrea di Rosa for his support and valuable information during the writing of my thesis. In addition, I would like to thank all the participants in the excavation of Myriam's Well beach in Tiberias in October-November 2022 whose attitude and assistance towards me were important.

Lastly, I am grateful to my family for their moral support during my postgraduate studies in Italy and Israel.

Ringraziamenti

Vorrei esprimere il mio ringraziamento al mio supervisore professore Emmanuel Nantet dell'Università di Haifa per il suo aiuto riguardo alla selezione del tema di ricerca e per il suo prezioso supporto durante la scrittura della mia tesi.

Inoltre, sono grato al mio secondo supervisore professore Michele Secco per il suo aiuto e prezioso consiglio durante le analisi chimiche e mineralogiche che si sono tenute presso l'Università di Padova.

Inoltre, sono grato alla mia professoressa Ruth Shahak-Gross per il suo aiuto durante le analisi con l'FTIR presso il suo laboratorio al Università di Haifa.

Esprimo inoltre il mio ringraziamento al Dott. Andrea di Rosa per il suo supporto e le informazioni preziose durante la scrittura della mia tesi. Sono anche riconoscente a tutti i partecipanti nello scavo della spiaggia di Myriam's Well a Tiberias ad ottobre-novembre 2022: il loro sostegno è stato molto importante.

Infine, vorrei ringraziare la mia famiglia per il loro supporto morale durante la mia laurea magistrale in Italia e in Israele.

Contents

List of Figures

List of tables

תַקצִיר

במהלך התקופה 2020-2022, האתר בחוף באר מרים בטבריה, ישראל, נחפר על ידי אוניברסיטת חיפה בהנחיית פרופסור עמנואל ננט. האתר מורכב משלושה מבנים שנחשפו לחלוטין: הרחבה של חומת העיר עם מזח הבטון, הבנוי מתחת למים בצד הצפוני של החוף., המבנה הארוך שנבנה לאורך שפת האגם והעמודים באזור E. החופרים הבחינו כי נעשה שימוש בטיט הידראולי לבניית חומת העיר וכמה קירות של המבנה הארוך. השימוש במרגמה הידראולית חוזר לתקופה הפרהיסטורית ובמיוחד בזמן המינואי והמיקני. תוספת של שברי קרמיקה או שאריות בעירה ממקור בעלי חיים העניקה תכונות הידראוליות למרגמות שהפכו אותן לעמידות בפני מים. מחקר תזה זה מורכב מניתוח כימי ומינרלוגי של חומרי המרגמה מהרחבת חומת העיר וחומות המבנה הארוך כדי לבחון את שלבי הבנייה השונים, מספר טכניקות בנייה והתפתחות השלבים הלא גבישיים במטריצת הקושר.

Sommario

Durante il periodo 2020-2021, il sito archeologico della spiaggia di Myriam's Well a Tiberias in Israel è stato scavato dall'Università di Haifa sotto la supervisione del professore Emmanuel Nantet. Il sito consiste in tre struttute che sono state rilevate completamente: l'estensione della mura della città con il molo subacqueo in calcestruzzo a nord della spiaggia, la Struttura Lunga costruita lungo la riva del lago, e le colonne dell'area E. Gli archeologi hanno osservato l'utilizzo di malta idraulica per la costruzione delle mura della città e alcuni tratti murari della Struttura Lunga. L'uso di malta idraulica inizia nel periodo Minoico e Miceneo. L'aggiunta di frammenti ceramici o residui di combustione di origine animale conferiva proprietà idrauliche alle malte, rendendole resistenti all'acqua. La presente ricerca consiste nell' analisi chimica e mineralogica delle malte provenienti del prolungamento della cinta muraria e dalle pareti della Struttura Lunga, per esaminare le diverse fasi costruttive, le diverse tecniche costruttive e lo sviluppo di fasi idrauliche scarsamente cristalline nelle matrici leganti.

Abstract

During the period 2020-2022, the site at Myriam's Well beach in Tiberias, Israel, was excavated by the University of Haifa under the supervision of Professor Emmanuel Nantet. The site consists of three structures which have been completely revealed: The extension of the city wall with the concrete pier, which is built underwater in the northern side of the beach., the Long Structure built along the lake shore and the columns in area E. The excavators noticed that hydraulic mortar was used for the construction of the City Wall and some walls of the Long Structure. The use of

hydraulic mortar goes back to the prehistoric period and specifically in Minoan and Mycenean time. The addition of ceramic fragments or combustion residues of animal origin gave hydraulic properties to mortars making them resistant against water. This thesis research consists on the chemical and mineralogical analysis of the mortar materials from the extension of the City Wall and the walls of the Long Structure, to examine the different construction phases, several building techniques and the development of the poorly crystalline hydraulic phases in the binder matrices.

1. Introduction

The city of Tiberias is located on the western side of the sea of Galilee in Israel. Excavations in the area have revealed that it was a multicultural and multireligious city from its foundation during the Roman period until the Ottoman occupation (Avni G. 2014, p. 72). The archaeological studies have also given an emphasis to the relationship of the city with the sea of Galilee. The lake is referred in the New Testament as one of the sites which was visited by Jesus. However, it was important for trading and economic reasons, since many activities were concentrated on the lake shore, and it was a way to move around Galilee by sailing.

The relation of the city with the lake is visible from the structures which have been revealed in the south of modern Tiberias on Myriam's Well beach. During the excavations of 2020-2022 carried out by the University of Haifa under the supervision of Professor Emmanuel Nantet, the structures were completely excavated and documented. The field works in Myriam's Well beach included underwater excavation as well as excavations on land. The site consists of three main structures: 1) The extension of the City Wall with the concrete pier which protrudes into the lake, 2) The Long Structure which develops along the Lake shore (Nantet E. 2020, p. 5, 2021, p. 4) and 3) The basalt and limestone columns in area E in the southern part of the beach. During the excavation seasons 2020-2022, the excavators tried to understand the function of the buildings and differentiate between different construction phases. The whole excavated area has also been mapped and documented. Moreover, the excavators focused on how the lake level fluctuations affected the development of the site and thus the construction of the City wall, the concrete pier and the Long Structure. The lake and its level fluctuations played a significant role in the life of Tiberias' residents. The level fluctuations obviously affected the construction of the City wall and the concrete pier which is underwater. The composition of the mortar materials and the construction technique of the concrete pier could possibly help us understand if the structures were underwater.

During the field work in Myriam's Well beach, the excavators noticed the use of hydraulic mortar with the addition of ceramic fragments especially in the area of the City Wall and the concrete pier. During the first two seasons (2020-2021), several mortar samples were selected from the City Wall and the concrete pier which is underwater in order to examine their chemical and mineralogical composition. During the last excavation season, I selected samples from all the walls and construction phases of the Long Structure. All the samples were studied and analyzed chemically and mineralogically at the facilities of the University of Padova and the University of Haifa in the framework of the Double Degree program between the two Universities.

The use of mortar was one of the most significant technological achievements of the humanity, since it was useful for structural purposes as well as for rendering and plastering walls and floors (Artioli G. et al. 2019, p. 166). The manufacture of hydraulic mortar with the addition of several aluminosilicate compounds, like ceramic fragments (Theodoridou M. et al. 2013, p. 3264) and/or combustion residues from organic matter (Regev L. et al. 2010, p. 3008, Lancaster L. C. 2012, p. 146), offered significant mechanical and durability properties to the mortar which made it resistant

against its contact with a water-saturated environment. The reaction between the lime and the aluminosilicate additives is called pozzolanic reaction. The pozzolanic reaction in the mortars consists of the dissolution and the precipitation of the aluminosilicate compounds in the alkaline saturated environment of the mortars and the formation of the poorly crystalline C-A-S-H phases in the binder matrix (Artioli G. et al. 2019, p. 170-171). This reaction is durable and can last for centuries after the setting of the mortar underwater. The addition of *pozzolana*, volcanic tuff and pumice from Phlegrean fields in the Gulf of Naples, gave improved properties and stability to the mortars which could be set underwater for the construction of moles and breakwaters (Jackson M. D. et al. 2014, p. 141). The mortar was placed in wooden cofferdams (formworks) which were put underwater. The wooden formworks could be built in situ or could be transferred like barges in the site of the construction and fill them with hydraulic concrete until they sink at the bottom of the sea (Vitr. 5.12.3, Brandon C. J. 2014, pp. 191-212).

In the case of Tiberias, the concrete pier was built in the same way, with wooden formworks which were built underwater and filled with concrete. However, there is no use of pozzolana in the mortars of Tiberias. The exploitation of pozzolana ceased during the Late Roman periods. On the other hand, hydraulic concrete is still in use during the medieval period with the addition of ceramics (cocciopesto).

Regarding the walls of the Long Structure, they are built mostly with the use of basalt stones and hydraulic concrete. The walls of the structure belong to different construction phases and the hydraulic concrete which was placed between the ashlars is heterogenous. The analysis of the mortar samples showed that except for the addition of ceramic fragments, there was the presence of combustion residues which was a common pozzolanic additive to the concrete in the Levantine region (Secco M. et al. 2022, p. 15).

1.1 Aim of the research

The aim of the mortars analysis is to determine the chemical and mineralogical composition of the hydraulic concrete both from the Long Structure and the City Wall. By the examination of the cement composition, we would be able to separate the buildings into different construction phases.

The studies in Myriam's Well mortars can also give us information regarding technological traditions. Tiberias is part of the Levantine region where the combination of different traditions in mortar technology was a common practice.

The structures built in the lake shore could be related with the lake level elevations. Nowadays the lake covers the concrete pier, and it is in close contact with the eastern part of the City Wall. The use of hydraulic mortar aimed at the protection of the structures against the lake.

Finally, the mineralogical and chemical analysis of the mortars could give us details about the new poorly crystalline phases (C-A-S-H) (M-A-S-H) which develop in the binder of the mortars after their setting in the structures.

2. History and Archaeology of Tiberias

The city of Tiberias was founded by Herod Antipas in ca 20 AD (Avi-Yonan M. 1950-51, pp. 167-168). It was a city which included a stadium, a theater, and a civic center (Avni G. 2014, p. 71-72). A *cardo* built with basalt slabs ran the length of Tiberias and was parallel to the shoreline (Hirschfeld Y. 1992, pp. 22-23). In the Byzantine period, Tiberias was a multicultural city including Jewish and Christian communities. At that period, the city was an important pilgrim center because of the basilica with the sacred anchor stone which was located on the top of Mount Berenice (Hirschfeld Y. 1999, pp. 241-242).

In the 7th century, the city surrendered peacefully to the Arab troops and became the capital and the administrative center of the province of Jund al-Urdunn. During the early Islamic period, the city maintained its multicultural and multireligious character. The archaeological excavations and surveys in the region have shown that the city expanded further to the south (Avni G. 2014, p. 75).

2.1. The archaeological site at Myriam's Well beach

The City Wall of Tiberias was built during Justinian's period, if we consider Procopius' text in his book, *De Aedificiis* (Procop. *Aed*. V.9.12.21). However, there are still Roman structural elements reused to the City Wall. The southern city gate belongs to the early imperial period when Herod Antipas founded Tiberias. The wadi channel with the vault which is close to the city gate is also attributed to the Early Imperial period of the city. The city wall is composed of basalt stone blocks well hewn in their exterior part and rough stones with hydraulic cement in the interior. It was 2.8 km long and surrounded the city from Mount Berenice to the lakeshore. The estimated height of the wall was 8-10m and the height of the towers was 12 m (Hirschfeld Y. 1999, p. 239). The wall was still in use until the 12th century when the residents of the city moved northwards to the Crusader's wall.

We can assume that the City Wall was connected to the structures of the Myriam's Well beach. The part of the City Wall which was built on the beach was useful for the protection of the city from the lake because enemy troops could also invade without a problem from the lake side. We can refer as an example the city of Magdala which was sacked by the Roman troops during the Jewish revolt where the Roman troops invaded from the lake side (Josephus, *De bello Iudaico,* III.10.5).

During my participation in the excavation in Myriam's well beach in Tiberias, I collected mortar samples from two main structures. The first structure was the city wall with the concrete pier which protrudes in the lake. This structure is located on the northern side of the beach. The concrete pier consists of six rectangular concrete blocks. The mortar of the blocks is a composition of lime, basalt and limestone aggregates and cocciopesto (ceramic) fragments as an artificial pozzolanic material. The concrete pier is below the lake level, whereas parts of the pier are above the lake level in summer. The next structure whose mortar was sampled and examined is the Long Structure. The Long Structure consists of several walls and construction phases and it is hollow at its southern end. Finally, the last structure which is located at the

southern side in Myriam's Well beach is the basalt and limestone columns. These columns are consisted of three parts. It is interesting to read the account of the Persian traveler, Nasir-i Khusraw who wrote about the presence of buildings in the lakeshore supported by columns made with marble (Nasir-i-Khusrau p. 17, Hirschfeld Y. 1992). These buildings could be associated with the basalt columns in area E in Myriam's Well beach. This text may show to us the relationship which the people of Tiberias had with the lake.

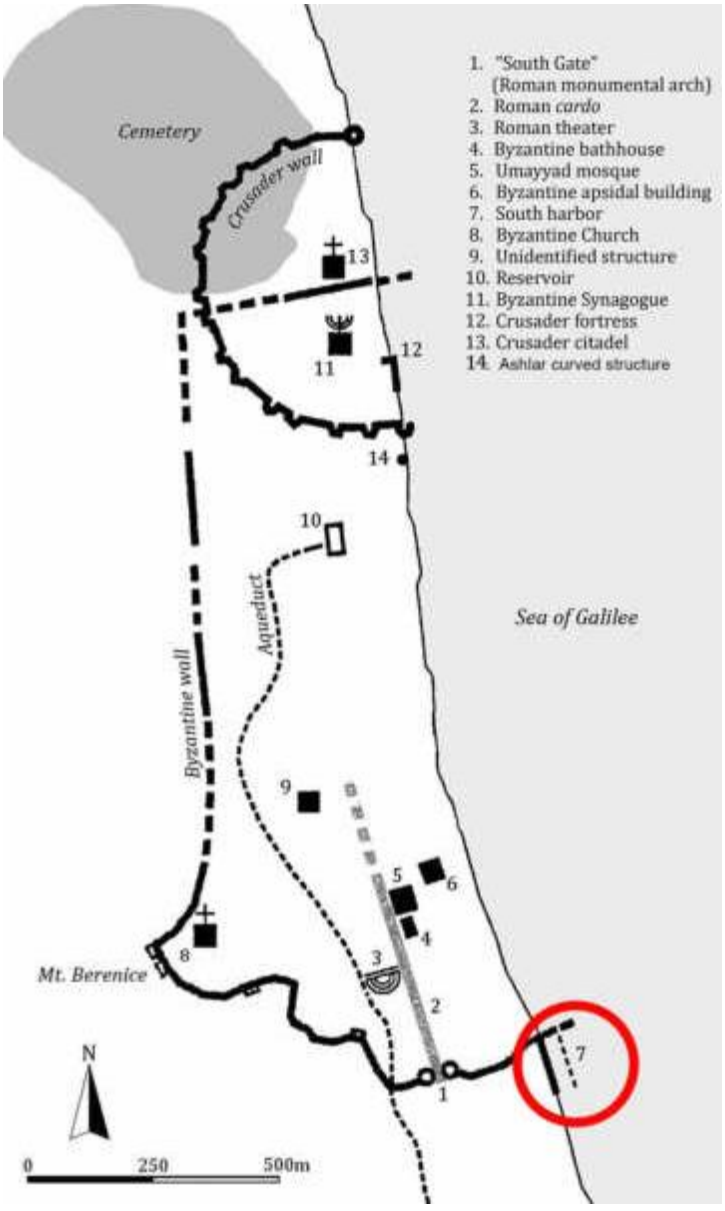

Figure 1. The city wall of Tiberias and the location of the site in Myriam's Well beach (E. Nantet 1992)

2.2. Description of the structures

2.2.1. The city wall

The extension of the City wall in the lakeshore is composed of two main walls, one built with limestone blocks (W1001) and the other with basalt blocks (W1002). According to the findings during the excavation season of 2020 and 2021, they can be dated to the Byzantine/Early Islamic period as the concrete pier. The city wall was built with regular ashlar blocks. Probably it was built in two phases, because we can notice different materials in the ashlar masonry. The extension of the city wall was built in order to protect the city from an invasion from the lakeside. The use of hydraulic concrete has been noticed between the junction of the ashlars.

The use of the pier built in the eastern side of the City wall, is unknown, and we can only make assumptions about the reason why it was built. The first assumption which we can make is that the pier was built as a continuation of the basalt city wall which is on the west in order to prevent the invasion of the enemy troops from the lake side. Another reason why the concrete pier was built was to support platforms which were quays of a harbor in Myriam's well beach. According to the ceramic findings, the concrete pier can be dated to the late Byzantine/early Islamic period.

It is interesting to describe the way the mortar blocks were set underwater. Wooden formworks were driven to the bottom of the lake and then the mortar in its slaked form was poured in the gap of the formwork. Vitruvius describes the construction of this kind of box in a very detailed way in his book *De Architectura* (Vitr. 5.12.2-6). Moreover, during ROMACONS project's research about the Roman maritime concrete, traces of the wooden planks in concrete piers and jetties were detected. For the construction of the wooden formwork, vertical piles (*destinae*) were driven underwater in order to support horizontal tie beams (*catenae*) (Brandon C. J. 2014 p. 191). Then, a couple of other vertical piles (*stipites*) were set around the *destinae* (Brandon C. J. 2014 p. 194). These piles supported the ends of the horizontal piles and the shuttering which was built around them.

There was also a second type of formwork which is described by Vitruvius. This type was constructed in situ, similarly to the previous one but it was watertight. The wooden walls of this formwork could be either single or double (Brandon C. J. 2014 p. 208). In some cases, when pozzolana was not available in some areas, builders used to cast non-hydraulic concrete in the double-walled formworks.

These types of formworks were common in the Roman republic and imperial times. We are not sure if this technique continued to exist in Late Antiquity and Byzantine times. Procopius of Caesarea describes a similar technique where wooden boxes were filled with rubbles and set underwater for the building of a new harbor in Constantinople (Procop. *Aed*. 1.11.18-20, Oleson J. P. 2014 p. 35). The term rubble may refer to hydraulic concrete, since Procopius was not possibly aware of the difference between mortar and rubble. Gertwagen tends to claim that the technique of the hydraulic mortar set underwater with the support of wooden formworks had disappeared during the Byzantine and Medieval period (Gertwagen R. 1988, p. 149). Byzantines did not acquire the knowledge regarding the construction techniques to build underwater structures and were not aware about the use of pozzolan in the

hydraulic mortar. Nevertheless, it is clear that the first technique described above or a similar one was still in use in the Sea of Galilee during the early Medieval period. However, the mortars used for the construction of the concrete pier differ from the mortars used for the construction of harbor structures during the Early Imperial period since there is no addition of pozzolana in our case study. The use of the wooden formwork can be related to the lake level fluctuations during the Byzantine/Early Islamic period. It is proof that the structure of the concrete pier was underwater during its construction at least partially.

Figure 2. Aerial photo of the extension of the city wall (W1001 and W1002) and the concrete pier (W1003) (Photo by J. Kim)

Figure 3. W1001 (Limestone wall). Southern facing (E. Nantet 2020)

Figure 4. Junction between the W1002 (basalt wall) and the w1001 (limestone wall) (Photo by E. Nantet 2021)

Figure 5. W1003 (Concrete pier) (Photo by J. Kim)

Figure 6. A square corner pile and a strake from the wooden formworks in the eastern most rectangular concrete block. Photo by A. Yurman

2.2.2 The Long Structure

The next building which has been analyzed was the Long Structure. During the excavation seasons, it was found out that it is composed of 17 walls in total with several building phases which run in a N-S axis along the lake shore. The architectural plan of the Long Structure was under research by the Master student Maxence Marques. Several structural elements protrude from the faces of the walls (E. Nantet 2020, p. 5, E. Nantet 2021, p. 4). There are two interpretations regarding the use of the Long Structure. Firstly, the Long Structure could be a harbor structure (Hirschfeld Y. 1992, pp. 27-30). Secondly, it can be a fortification connecting Tiberias and Hammat Tiberias, which could have become later a seawall protecting the city of Tiberias from the lake (Stepansky Y. 2017, map 39, no 98). However, it is difficult to determine the real use of the building, since it consists of many building phases and it is hollow in its southern side composed of different spaces and rooms, which rejects its use as a sustaining wall. The Long Structure was also built with the use of hydraulic concrete and basalt and limestone ashlar blocks in most of its parts.

Going from north to south, the first wall of the Long Structure (W2001) is located at short distance from the extension of the City Wall. The wall is built along the lakeshore with basalt ashlar blocks and mortar. A part of this wall has the shape of a door which was closed with basalt blocks of smaller size. On the eastern side of the door structure, there are two steps constructed with basalt stones connected with mortar.

Figure 7. W2001 (photo by M. Marques)

Figure 8. W2001 “Door” section (photo by Konstantinos Thomas)

In the southern end of the w2001, there is another wall (W2002) vertical to the former one. This wall is connected with the wall 2003 which was built along the lakeshore. Possibly these walls (W2002 and W2003) belong to the same construction phase, since they were built with the same building technique with irregular basalt and limestone blocks with hydraulic mortar among them.

Figure 9. W2001 on the right side, W2002 vertical to the W2001 and W2003 on the left side (Photo by M. Marques)

In the southern end of the W2003, there are two walls (W2004-W2005) parallel to each other protruding to the lakeshore. Their building technique seems similar to the W2003 and W2002. Behind these walls, there is another wall (W2006) built with regular ashlar basalt blocks. The specific wall was built in two distinct layers which may belong to different building phases. The lowest layer is composed of huge basalt blocks whereas the highest layer includes basalt blocks of smaller size.

Figure 10. W2004 (on the right) on the south and W2005 (on the left) on the north (photo by K. Thomas)

Going further to the south of the beach, we can notice the presence of two parallel walls (W3004-W3006) protruding to the lakeshore and connected with the W3005. Their building technique with irregular basalt blocks and hydraulic mortar seems similar and they may belong to the same construction phase. In the eastern end of the wall W3004, there is a connected wall (W3002) built along the lakeshore. Attached to this wall on its northern side there is a pavement constructed with basalt stones and concrete. At the southernmost end of wall W3002 there is a wall (W3003) connected to it and built with pierced ashlar blocks and cubic blocks. These pierced blocks might belong to the aqueduct of Tiberias which was destroyed during the Early Islamic period.

Figure 11. W3006 on the right (north), W3005 horizontal in the middle and W3004 on the left (south). Aerial photo by M. Marques

Figure 12. Aerial view of the W3002 (Photo by M. Marques)

Figure 13. W3002 (Photo by K. Thomas)

Figure 14. W3001 on the left side and W3003 (aqueduct stones) on the right (Photo by M. Marques)

Figure 15. Pierced ashlar (Aqueduct) stone from the W3003. (Photo by K. Thomas)

Figure 16. Fallen block from the W3003. (Photo by K. Thomas)

Behind the wall W3002, there are three walls perpendicular to it (W3001, W3010 and W3011). These walls divided this part of the Long Structure in multiple rooms. They are built with regular ashlar masonry and are plastered. Lastly, in the south side of the Long Structure we have noticed the presence of a sewer constructed with two short walls (W3008-W3009). It seems that the mortar of the sewer has a brownish color because it is composed of clay. Behind the sewer and on the western side, there is another wall (W3007) which is built with regular basalt blocks.

Figure 17. The sewer of the Long Structure, W3008 on the right, W3009 on the left and W3007 behind the sewer (Photo by M. Marques)

3. State of the art

3.1 Written sources

The first written source where there is a mention regarding the technology of the mortar is the treatise *De Lapidibus* written by Theophrastus in the 4th century BCE. In his work, Theophrastus refers to the slaking of the mortar with the use of a stick and without the use of hands (Theo. *De Lap*. 66; Oleson J. P. 2014, p. 12). In the imperial period, Pollux refers to a comment in Theophrastus treatise, *On metals*, about the *salax* which was a sieve used in ore activity (Poll. *Nomen.* 10149). The same tool was used by the Romans to remove particles from the hydrated lime or the volcanic pozzolana in preparation of slaking the mortar (Oleson J. P. 2014, p. 12).

In his work, *De Architectura,* Vitruvius provides a detailed description about the cast of hydraulic concrete and the building of harbors. More specifically, he refers to the difficulty of transportation of the raw materials to the site of construction (Vitr., 1.2.8). He also mentions the ratio of mixing between the lime and the inert. The ratio should be three parts of quarry sand and one part of lime. If quarry sand is not available sea or river sand should be used in the ratio of two to one.

In a next passage, the author refers to the proper selection of lime for the manufacture of mortars. The stone should be dense and compacted in order to use for concrete work. On the other hand, porous stone can be used only for plastering (Vitr., 2.5.1). The Roman writer does not forget to mention one more time the ratio of mixing between the lime and the inert. In the case that river or sea sand is mixed with lime, one part of ceramic fragments should be added (Vitr., 2.5.1). The ceramic fragments or powder offers great mechanical and hydraulic properties to the mortars as we will mention below.

The next passage is the most important in order to understand the cast of hydraulic mortar with the use of pozzolana. In this passage, Vitruvius writes about the *Pulvis Puteolanus* which is quarried in the region of Baiae and around the volcanic district of Vesuvius (Vitr. 2.6.1). Pulvis means powdery sand and the word *puteolanus* defines the origin of this material from the city of Puteoli (today Pozzuoli) in the Gulf of Naples. The term which is used today for the volcanic ash from the Bay of Naples is pozzolana. Vitruvius mentions the hydraulic properties of the mortar mixed with pozzolana (Vitr. 2.6.1). When lime is mixed with pozzolana in a water-saturated environment, there is a reaction which makes the composite material resistant to water erosion. In a next passage (Vitr., 2.8.2), Vitruvius writes regarding the proper hydration of the hydraulic mortar.

Lastly, Vitruvius makes reference to the building techniques of harbors with hydraulic concrete. For the construction of moles, it is necessary to build a wooden formwork with beams and piles which would be placed underwater (Vitr., 5.12.3). After the construction of the formwork, the slaked mortar can be poured in the empty space of the formwork. Another technique which is described by Vitruvius is the construction of a double walled formwork. A double walled cofferdam was built in situ and the water was pumped out, so it remained dry. This technique was useful only when pozzolana was not available (Vitr., 5.12.3).

Strabo, in his book *Geographia*, made a reference to the construction of the ancient harbor of Pozzuoli which is 200 km far from Rome (Str., *Geo*. 5.4.6; Oleson J. P. 2014 p. 24). He gives emphasis on the hydraulic properties of the mortar mixed with pozzolana earth.

Another writer who mentions the properties of hydraulic concrete and the mixing with pozzolana is Pliny the Elder. In his work, *Historia Naturalis*, Pliny describes the construction of one of the breakwaters in Portus, the harbor of Rome, with hydraulic mortar mixed with pozzolana from the Gulf of Naples (Pl., *HN* 16.201-202). In another passage (Pl., *HN* 36.70), he describes one of the building techniques which were used for the construction of harbors in the open sea, like the harbor of Caesarea Maritima. In this passage, he mentions the building of two towers in ships (probably he means the barges which carried the mortar) which were sunk at the point of the construction. Like Vitruvius, Pliny the Elder refers to the addition of ceramic fragments in the mortar (Pl., *HN* 36.175). Ceramic fragments were considered an artificial pozzolanic material with similar properties as pozzolana.

There is no reference about the use of pozzolana in concrete during the Byzantine period. There is only one reference of the historian Procopius in his book, *De Aedificiis*, about the construction of a harbor in Constantinople. The moles of the harbor were built with the use of wooden boxes, called kibotoi, which were filled with rubble and sank underwater (Procop., *Aed*. 1.11.19).

3.2. Scientific research on hydraulic mortars

According to scientific research about composite materials, the use of hydraulic mortar started in the Aegean world during the Bronze Age. Since the utilization of pozzolana was not known, artificial pozzolanic materials, like crushed ceramics, were used instead. Ceramics are also an aluminosilicate compound which can react with lime and water and create the insoluble C-A-S-H phases (calcium aluminosilicate hydrates). As an example of the first application of the hydraulic mortar, we can refer to the case of Cyprus where hydraulic mortar was manufactured with the addition of ceramic fragments and was applied in buildings of the Late Bronze Age (Theodoridou et al. 2013, p. 3264). Mortar samples from floors, baths, water canals, wells and external wall finishes coming from various Late Bronze Age monuments were collected and examined by means of petrographic microscopy, SEM-EDS, XRPD and XRF. After the analysis, it was noticed that the ceramic fragments offered hydraulic properties on the mortars (Theodoriodou M. et al. 2013, p. 3265-3267). The scholars have detected the presence of reaction rims which is the result of the reaction between the aluminosilicate compounds and lime in a saturated environment. Moreover, the presence of C-A-S-H phases which were detected by means of XRPD and SEM examination is another proof of the utilization of ceramic fragments in the lime mortars.

The use of hydraulic concrete in its initial stages was not limited only in Cyprus and the Aegean world. Plasters from the site of Tell es-Safi/Gath of the Iron Age were analyzed in order to find out the mineralogical and chemical composition. The results of the analyses showed the presence of silicates which are associated with the ceramics and hydroxilapatite (Regev L. et al. 2010, p. 3008-3009). Hydroxilapatite is

related to the use of organic materials. Organics were used in the mortars as artificial pozzolanic materials although their presence in the Tell es-Safi's mortars was probably accidental.

Lancaster's research on the ash mortars in North Africa showed that builders mixed ash from wheat, grass and herbivore manure with lime in order to produce hydraulic mortar to line cistern (Lancaster L. C. 2012, p. 149). He also proved with experimental studies that the ashes from the herbivore manure can produce more C-S-H when they are mixed with the lime compared to the ashes from the grass and the wheat (Lancaster L. C. 2012, p. 147).

Another significant research was carried out by Maravelaki-Kalaitzaki P. et al. 2003. The scholars have selected 28 mortar samples from several Cretan monuments which are dated from the Minoan until the modern period. The purpose of their study was to examine different mortar technologies. The samples were measured by means of Optical Microscopy, XRPD, Thermal analyses, Calcimetry and FTIR. Their results showed that mortars were prepared by the use of sea sand or calcareous stones. Traces of feldspathoids and pyroxenes is an indicator that pozzolana was added in the mortars. Also, the C-A-S-H phases were developed in the mortar matrix which is the result of the pozzolanic reaction between the aluminosilicate compounds and the lime. Traces of diopside, leucite and analcime indicate the presence of pozzolana of volcanic origin. Probably the Cretan builders had access to Santorini's earth, a pozzolanic material with similar quality as the pozzolana from Campi Flegrei.

3.3. The research projects on the hydraulic mortar in Caesarea

However, hydraulic concrete was not used for the construction of harbors until the Late Roman Republican times. Hydraulic mortars were mostly used in the masonry of the buildings and as rendering in the walls. In the second century BCE, hydraulic concrete with the utilization of pozzolana from Campi Flegrei was applied in harbor structures (Oleson J. P. and Jackson M. D. 2014, p. 3). ROMACONS project has collected long mortar cores from several Roman harbors in the Mediterranean Sea and examined the chemical and mineralogical composition of their samples (Brandon C. J. and Hohlfelder R. L. 2014, p. 39). The volcanic tuff and pumice from Campi Flegrei are pyroclastic rocks which came from the volcanic eruption of the Neapolitan Yellow Tuff, approximately 15000 years ago (Jackson M. D. et al. 2014, p. 150). ROMACONS team has analyzed the concrete cores by means of XRPD, SEM-EDS, Petrographic examination and XRF. Their results were valuable in understanding the chemical and mineralogical composition of the hydraulic mortar with the occurrence of volcanic tuff and pumice as coarse and fine aggregates. Through their chemical and mineralogical analyses, the ROMACONS team has studied the chemical reactions and the alteration products in the maritime mortars. Al tobermorite is one of the main C-A-S-H phases in the hydraulic concrete (Jackson M. D. et al. 2014, p. 142-143). This phase is developed in relict lime clasts, in the binder matrix, in the pozzolanic aggregates and as fabrics in the voids. Some other important minerals which are formed during the pozzolanic reaction between the volcanic pumice and the lime are hydrocalumite, ettringite and zeolite. The first two minerals are developed because of

the presence of sulphate and calcium chloroaluminate phases. The last ones could be formed in the voids of the mortar as alteration minerals (Jackson M. D. et al. 2014, p. 143). The examinations on Roman maritime concrete showed a composition of broken ceramics (Jackson M. D. et al. 2014, p. 114) which replaced in some cases the pozzolan fragments due to the unavailability of the latter ones.

One of the most important research projects of ROMACONS was the analyses of the concrete cores from Sebastos harbor in Caesarea Maritima, Israel. 5 long cores have been collected from the breakwater of the harbor. After a macroscopic examination on the mortar cores, the team has detected the presence of Kurkar aggregates, a local calcarenite, which was added in the lime mortar as a coarse aggregate. Moreover, fine tuff and pumice aggregates have also been added to the mortars making the composite material waterproof (Holhfelder R. L. and Brandon C. J. 2014, p. 77). The samples contained ceramic (cocciopesto) fragments which replaced the pumice aggregates, since the latter were not in large quantities. Furthermore, the team has analyzed the cores by means of Optical microscopy, Scanning Electron Microscopy-Energy Dispersive Spectroscopy (SEM-EDS), X-ray Fluorescence (XRF) and X-ray diffraction (XRD). At the same time, they measured with the same methods volcanic tuff fragments from the area of Bacoli in the Gulf of Naples in order to examine the provenance of the tuffs in Caesarea's mortars. The results showed that the tuff fragments in the mortars had a composition typical for pyroclastic rocks, with the occurrence of sanidine and clinopyroxene, similar to the composition of the tuffs from Bacoli (Vola G. et al. pp. 327-330). This way, the team has discovered the provenance of the volcanic material in the mortars. Moreover, the presence of zeolitic minerals as altered minerals was noticed. Zeolites filled the pores of the mortars. The most significant mineral phases which were found out during the analysis were poorly crystalline C-A-S-H phases (calcium-alumino-silicate-hydrates) (Vola G. et al 2011, p. 332). These mineralogical phases have been indicative in every hydraulic mortar and they form as a result of the reaction between the pozzolanic material (artificial or natural) which is an aluminosilicate compound with the lime in a water-saturated high alkaline environment. The C-A-S-H phases mainly develop in the binding matrix or in the area of reaction rims between the pumice aggregates and the matrix.

Compared to the quality of Sebastos' mortar, the mortars from the Italian harbor structures are better. Sebastos harbor was built in the open sea exposing in this way the mortar structures to the strong waves and current of the sea environment. Furthermore, Levantine builders who were not experienced with the manufacture of the hydraulic concrete worked in Caesarea's harbor. Last but not least, the use of Kurkar as a caementa (coarse aggregate) was not a suitable choice, as it made the material more porous.

Another study which is related to the chemical and mineralogical composition of Caesarea's mortars was carried out by Secco M. et al. 2022. Secco et al. have selected samples from Caesarea's harbor (Area K) as well as from structures on land. The samples have been analyzed by means of XRPD quantitative analysis, ^{29}Si and ^{27}Al Magic-Angle Spinning Solid-State Nuclear Magnetic Resonance, FTIR analysis, Total Organic carbon (TOC) and isotopic analysis (C^{13}). After the XRPD analysis, the research team has clustered the samples in homogeneous mineralogical groups

through the multivariate statistical method PCA (Principal Component Analysis). According to their chemical and mineralogical composition, mortars were divided into three different recipes. The first recipe contains mortars whose pozzolanic and carbonation reaction are strong with the former one to prevail over the latter one slightly. The second mortar recipe includes binders which have a pozzolanic reaction much more intense than the carbonation reaction. The scholars have noticed the presence of M-A-S-H phases (magnesium-alumino-silicate hydrates). The presence of magnesium in the mortars can be justified by their reaction with the seawater. The third mortars' recipe shows a more balanced ratio between the carbonation and pozzolanic reaction.

The mineralogical and chemical analyses in Caesarea's mortars indicated that there was an addition of combustion residues in the binders. Since pozzolana was not available in large quantities, Levantine builders made use of combustion residues which is a silicate material reacting with lime. The addition of ash in mortars was a Phoenician technique which was still in use in the mortars of Sebastos' harbor. Consequently, there was a combination of building techniques, on one hand the use of pozzolana was a Latin technique for the manufacture of maritime concrete and on the other hand the addition of ash and charcoal in the mortars consisted of an eastern technique used by Phoenicians in the masonry and the rendering of the walls.

3.4. The hydraulic mortar in Tiberias

Three main structures were excavated in the Myriam's Well beach in Tiberias and were built with the use of hydraulic concrete. The mortar was manufactured with lime, basalt and carbonate aggregates. Several mortars also showed the presence of ceramic fragments and powder. As it was mentioned above, both Vitruvius and Pliny mention to the addition of crushed ceramics in the mortars which were more available compared to the volcanic ash and pumice. Except the addition of crushed ceramics in the binder, the builders in Tiberias' structures might have added combustion residues as well. The use of combustion residues in the mortars in the Levant was common from the Phoenician period. Charcoal was also present in Tiberias' mortars, but it was probably the remain of the coal which was placed in the kiln to burn the limestone. Lancaster suggests that charcoal cannot be used as a pozzolanic additive, even though it contains silica, because it reacts very little with the lime (Lancaster L. C. 2012, p. 147). Pozzolana has not been found in Tiberias' binders. The use of pozzolana might have been forgotten during the Late Byzantine/ Early Islamic period (Gertwagen R. 1988, p. 149) when the structures can be dated.

In the case of Tiberias, we should take into consideration the construction technique of the wooden formworks. The sixth concrete block in the pier of Myriam's Well beach contained parts of the wooden formwork which was used to set the concrete underwater. According to Gertwagen, Procopius refers to the use of rubbles instead of hydraulic concrete in chests, which are named *kibotoi*, for the construction of moles and breakwaters (Gertwagen R. 1988, p. 149). Also it should be considered that Byzantines were not specialized in the construction of underwater structures with the use of concrete. There is an absence in harbor structures built with hydraulic concrete and dated to the Byzantine period. On the other hand, the case of Tiberias is an exception since we can clearly notice the use of hydraulic concrete for the underwater

structure of the pier. Hohlfelder comments on the same Procopius' passage suggesting that the Byzantine historian wanted to describe the same construction technique used in the Early Imperial period (Holhfelder R. L. 1988, pp. 57-58). The structures in Myriam's Well beach can be dated to the Late Byzantine/Early Islamic period, according to the ceramic and glass findings (Nantet E. 2020, p. 4, Nantet E. 2021, p. 5). Consequently, Byzantines were aware of the qualities of the hydraulic mortar and its use in harbor structures, whereas they were not specialized in the use of natural pozzolans, like Roman builders and engineers.

4. Sampled Areas

150 samples of binding materials were selected and 66 of them were analyzed from all the structures in Myriam's Well beach in Tiberias. The complete list of sampled material is reported in Tables 1 and 2.

Wall	Samples	FTIR	XRPD bulk analysis	SEM-EDS	OM	XRPD Binder analysis	SEM EDS binder analysis
1001 A6	1001_A6s1	X					
	1001_A6 S2	X					
	1001_A6 S3	X					
	1001_A6 S4	X					
1002 A3	1002_A3 s1	X					
	1002_A3 s2	X	X	X	X	X	X
	1002_A3 s3	X					
	1002_A3 s4	X					
	1002A3 s5	X					
	1002_A3 s6	X					
	1002_A3 s7	X					
	1002_A3 S8	X					
1002 A5	1002_A5 S1	X					
	1002_A5 S2	X					
	1002_A5 S3	X					
1002 A9	1002_A9	X					

1002 D	1002_Ds1	X					
	1002_Ds2	X					
	1002_DS3	X	X	X	X	X	X
	1002_DS4	X					
1003 (concrete pier)	1003 s1	X					
	1003 s2	X	X	X	X	X	X
	1003 s3	X					
	1003 s4	X					

Table 1. Mortar samples from the the City Wall, including the concrete pier (W1001, W1002, W1003).

Walls	**Samples**	**FTIR**	**XRPD bulk analysis**	**SEM-EDS**	**OM**	**XRPD binder analysis**	**SEM-EDS binder analysis**
2001	2001 "door"	X	X	X	X		
	2001F206	X					
	2001F207	X	X	X	X		
	2001s1	X	X	X	X		
2003	2003s1	X	X				
	2003s2	X	X				
	2003s3	X					
	2003s4	X					
2004	2004s1	X	X	X	X	X	X
2005	2005S1	X	X	X	X		
2006	2006s1	X					
	2006s2	X	X	X	X	X	X
	2006s3	X					
	2006s4	X					
	2006s5	X					
	2006s6	X					
3001	3001s1	X	X	X	X		
3002	3002s1	X	X	X	X	X	X
	3002s2	X					
	3002s3	X					
	3002s4	X					
	3002s5	X					
Pavement in 3002	3002_P	X	X				
3003 Aqueduct stones	3003_AQ s1	X	X	X	X	X	X
	3003_AQ s2	X					
	3003_AQ s3	X					

	3003_AQ s4	X					
3003 Fallen blocks	3003_FB s1	X					
	3003_FB s2	X					
	3003_FB s3	X	X	X	X		
	3003_FB s4	X					
3004	3004s1	X	X	X	X		
3005	3005s1	X	X	X	X	X	X
3006	3006s1	X	X				
	3006s2	X					
	3006s3	X					
3008-3009 (sewer)	3008-09s1	X					
	3008-09s2	X	X	X	X		
	3008-09s3	X					
3010	3010s1	X	X	X	X		
3011	3011s1	X	X	X	X	X	X
L327	L327	X	X	X	X		

Table 2. List of mortar samples from the Long Structure.

4.1. Mortar samples from the city wall and the concrete pier

The first structure which was sampled is the City Wall (walls 1001 and 1002), including the concrete pier (W1003) which protrudes into the lake. More specifically, mortar samples were taken from the parts of W1002 which were excavated in trenches A3, A5, A6, A9 and D. Trench A3 was opened in the northeastern side, A5 is located on southeastern side of the wall, A6 is on the northern side of the limestone wall 1001 and trench A9 was excavated in the northern side of the basalt wall 1002. Trench D is located on the eastern side of the basalt wall 1002. The composition of these mortars and their hydraulicity may be associated with the lake level elevations, since the mortars used for the construction of these structures should be hydraulic in order to resist the erosion of the water.

4.2. Mortar samples from the Long Structure

Following the description of the Long Structure from the north to the south, the first structure which was sampled was the wall 2001. The "door" section and the steps in the eastern side were sampled as well in order to examine any similarities between the mortar samples of the wall 2001. Secondly, the walls 2002 and 2003 were sampled all along their range. The concrete of these walls seems quite heterogeneous. Next structure which was sampled was the wall 2006 which seems to be similar to the first wall, 2001. Moreover, the walls 3004, 3005 and 3006 were sampled to examine the similarities in their chemical and mineralogical composition, since I consider them to belong to the same construction phase. Going more to the south, the wall 3002 and the pavement excavated in the north of the wall were sampled. At the southernmost section of the Long Structure, I collected samples from the walls 3010 and 3011 which separate this section in different spaces. These samples included pieces of both mortars and plasters. The plaster found in L327 in the vicinity of the wall 3010 was

analyzed too. The wall 3003 built with the pierced ashlar blocks (aqueduct stones) and the cubic ashlar blocks on the top of them were sampled as well. Some of the cubic blocks fell because of visitors' disturbance in the archaeological site. Last samples were collected from the walls 3008-3009 whose composition is a mixture of lime and clay. These walls have been identified by the excavator as a possible sewer.

Figure 18. From the left to the right: samples s2001_F206, 2003s1, 2006s2, s3001, 3002s5. Photo by K. Thomas

Figure 19. From left to right: 3003_AQs1, 3003_FBs2, s3004, 3006s3, 3008-09s2.

Figure 20. 1003s1 on the left and 1002_Ds1 on the right.

5. Materials and Methods

The samples were taken through manual removal by means of chisels and hammers during the excavation seasons 2020, 2021 and 2022. The analyses of the mortar samples were carried out in the facilities of the University of Haifa and the University of Padova in the framework of the Double Degree Master program between the two Universities.

5.1. Macroscopic examination and FTIR

Firstly, the samples were examined through a macroscopic view in order to determine the nature of the aggregates and the lime matrix. Later, the samples were examined through the method of FTIR (Fourier Transform Infrared Spectroscopy). FTIR method is used to find out the major mineralogical composition of the samples (Weiner S. 2010, p. 275). We may detect the main mineralogical phases, like carbonates, silicates, etc. (Baragona A. et al. 2022, p. 506). It can also be used to determine the hydraulicity of the mortar samples and the organic matter in the binders. The method is relatively simple and it takes some minutes to get our results. In Transmission mode, we should mix 3 mg of our material with 250 mg of potassium bromide in an agate mortar forming in this way a powder. Then the powder is pressed in a Pike Press to produce 5 mm pellets. The disk which is created is brought into the Thermo iS5 spectrometer. 32 scans were recorded over the range 4,000-400 cm^{-1} with a spectral resolution of 4 cm^{-1} (Weiner S. 2010, pp. 276-277). Before we collect the spectra of our sample we should select the background spectrum.

5.2. XRPD on bulk samples

Later on, 23 of the representative samples were chosen and analyzed by means of XRPD (X-ray Powder Diffraction), SEM-EDS (Scanning Electron Microscopy-Energy Dispersive Spectroscopy) and Optical Microscopy.

The XRPD-QPA analysis took place in the facilities of the Department of Geosciences at the University of Padova, Italy under the supervision of Professor Michele Secco. Before the XRPD analysis, the mortar samples were subject to micronization by a McCrone Mill, using a plastic jar with zirconia grinding elements and ethanol as micronizing fluid. After the micronization, we waited for 24h to dry the samples. When the samples got dried, I homogenized each sample with 20wt% of ZnO in an agate mortar for the quantification of the paracrystalline fraction (Dilaria S. et al. 2023, p. 572). Then, the mixture powder was placed in a disc which was set into the diffractometer.

For the XRPD-QPA analysis, a Malvern PANanalytical X' Pert Pro diffractometer was used with a real time multiple strip detector. Data acquisition was carried out by the use of a continuous scan in the range 3-85 [2θ] with a virtual step scan of 0.02 [2θ] (Secco M. et al. 2022, p. 3, Dilaria S. et al. 2023, p. 572). The interpretation of the data acquired through XRPD was carried out through High Score plus (qualitative analyses) and TOPAS software (Quantitative analysis). The data from the quantitative data are presented in the Table 3. I also took advantage of the Profex software as an additional tool for the qualitative analysis of the samples and the identification of the phyllosilicate gels (smectite like).

5.3. Colorimetry

Moreover, colorimetry measurements were applied to determine thee colors of the mortar powders. Colorimetry is a non-destructive method used to evaluate the chromatic parameters of an object. It is an important method for the conservation studies and the restoration of the mortars. Colorimetry measurements use three parameters to determine the color differences: L* which is associated with the lightness of the color, a* which is relevant to the red-green axis of the color and b* which related to the yellow-blue axis of the color (Navarro-Mendoza E. G. et al. 2023, p. 2589). Moreover, I measured the RGB values (Red, Green, Blue) extrapolated from the L* a* b* ones. For this method, I used an Android application to examine the colors of all the powdered samples in order to differentiate between different color groups of mortars. Therefore, we can perform a first preliminary recognition of the distinctive construction phases of the Long Structure.

5.4. Optical Microscopy

Furthermore, I performed a petrographic study on representative samples from each wall of the "Long Structure" and the "City Wall". The petrographic study was carried out with the use of Transmitted Light Optical Microscopy on 30 μm thin sections, obtained by vacuum impregnating portions of the materials with epoxy resin (Secco M. et al. 2020 p. 64). The optical microscopy study was performed with the use of a Leica DM790 microscope at the facilities of the Department of Cultural Heritage at the University of Padova. Through the Optical microscopy study, we clustered the

samples in different groups according to their composition, both in relation to the aggregates and their binder. I also examined the presence of lumps, the porosity and the additives in the binder.

5.5. SEM-EDS

After the analysis by optical microscopy, the thin sections were microchemically characterized by SEM-EDS (Scanning Electron Microscope-Energy Dispersive Spectroscopy). We made use of COXEM EM-30 AX PLUS at the facilities of the University of Padova. The SEM-EDS was equipped with a tungsten cathode and a four-quadrant solid state BSE for imaging. The analytical conditions were: accelerating voltage 20kV; filament current 1.80A; emission current 20μA; aperture current 300nA; working distance 20-30mm; (Secco M. et al. 2019, p. 268, 2020, p. 65, 2022, p. 3). More specifically, I searched for the elemental composition of the binder matrix and the reaction rims around the aggregates. Moreover, I determined the composition of some aggregates. The SEM analysis was carried out in BSE (Backscattered Electrons) mode.

5.6 XRPD and SEM-EDS analysis on the binder fraction

Finally, the multianalytical characterization of the mortars was complemented with a mineralogical-spectroscopic study of the binder fractions of nine selected samples from the City Wall and the Long Structure to determine the reactivity properties of the binding mixtures and the extent of the pozzolanic reaction processes (Secco M. et al. 2020, p. 66). In order to separate the binder fraction, I made use of the Cryo2Sonic 2.0 method. Firstly, the binder was mechanically separated from the rest of the components. Then, I placed the samples in cylinders in which I added a sodium hexametaphosphate to favor the suspension of the fine binder which tends to flocculate. After this procedure, the samples were sonicated in an ultrasonic bath. For the sonication process an Elma s60 Elmasonic was used. Later the samples were centrifuged in a Rotina 380. Then, they were suspended in ultrapure water for 20 hours in order to obtain a dimensional separation, since the binder particles which are smaller than 5 μm would flocculate on the water (Addis A. et al. 2019, p. 377). Finally, the upper part is sampled which is sonicated and centrifuged again and is left to dry for 24 hours. After the separation process, the binder part was examined by means of XRD and SEM-EDS analysis in BSE mode to examine the extent of the carbonate and the pozzolanic reaction in the matrix.

Finally, we performed a statistical treatment on the quantitative data from the XRPD and SEM-EDS by means of PCA (Principal Component Analysis). With this method, the samples were separated into distinctive groups according to their mineralogical and elemental composition.

6. Results

6.1. Macroscopic view

The samples were examined through a stereomicroscope to see the aggregates and the binder matrix. The mortar samples seem heterogeneous to each other. Most of the aggregates which were added are basalt fragments which probably were supplied in

the area around Tiberias, since there are relevant basalt outcrops. Limestone and quartz aggregates were also present in the composite materials. Ceramics were added as an artificial pozzolanic material and are visible as reddish inclusions in the binders. In some cases, charcoal fragments have been noticed as well. The presence of charcoal may be associated to combustion residues which was a common pozzolanic material rich in amorphous silica. However, it may come from the calcination process of the lime from the charcoals which were used in the lime kilns.

Figure 21. Sample 2001 “door” (left) and sample 2001_F207 (right). Image under stereomicroscope.

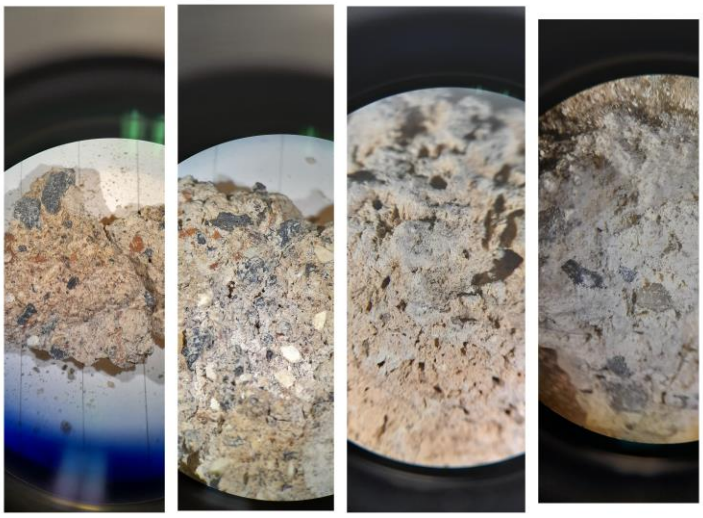

Figure 22. From left to right; s2004, s2005, s3001, 3002s1. Image under stereomicroscope

Figure 23. Sample 3003_AQ. Image under stereomicroscope

Figure 24. Plaster found in L327 (close to W3010). Image under stereomicroscope

Image 25. Sample 3008 (sewer). Image under stereomicroscope

6.2. FTIR results

The mortar samples are mainly composed of calcite. The absorption peaks at 1425 cm^{-1} (v3), 712 cm^{-1} (v4), 875 cm^{-1} (v2) correspond to the vibrational mode of the anthropogenic CO_3 (Sekhaneh W. A. et al. 2020, p. 167, Asscher Y. et al 2020, p. 533 Table 2). The first peak (v3) corresponds to the asymmetric stretch, the second one (v4) is related to the in-plane bending and the third one (v2) to the out of plane bending vibrations of CO_3 (Maor Y. et al. 2023, p. 2). The peaks at 1630 (v2) and 3340 cm^{-1} (v1) are associated with the OH bending vibration in water (Puertas F. et al. 2011, p. 2049). The peaks between 950 and 1100 cm^{-1} correspond to the asymmetric stretching vibration in the Si-O bond (v3) in the SiO_4 (Sekahaneh W. A. et al. 2020, p. 166) which is included in the C – S – H gel (Horgnies M. et al. 2013, p. 256) and the basalt and quartz aggregates. The peak at 460 cm^{-1} is relevant with the SiO_4 bending mode (v4) (O – Si – O) (Puertas F. et al. 2011, p. 2047, Secco M. et al. 2022, pp. 12-14).

All the samples show strong peaks of calcite which means that the carbonate phases are quite relevant. The peaks in the silicate group are important but only in a few examples overcome the peaks of the carbonate phases. This result indicates to us that there was a pozzolanic reaction in the binder matrix between the lime, the water and the aluminosilicate compound, likely due to the occurrence of the ceramic fragments which are additives in the concrete of the city wall. The hydraulic reaction is related to the formation of C-A-S-H gel-like phases in the binding matrix. It is also responsible for the formation of reactive rims with a composition of C-A-S-H around the lime clasts and the pozzolanic aggregates (Pecchioni E. et al. 2014, p. 12). However, the presence of the reaction rims can be detected with the methods of SEM-EDS and Optical Microscopy. The silicate peaks are also attributed to the presence of

quartz and basalt, since these minerals and rocks were added as an inert to the binders of the Myriam's Well beach.

The samples with the strongest peaks in the silicate groups were the samples which come from the City Wall and the concrete pier (W1002 and W1003). The silicate peak in these samples is related to the formation of C-A-S-H and M-A-S-H in the binders. The sample which was taken from the limestone wall (w1001) showed a more pronounced peak in the calcite group rather than silicates.

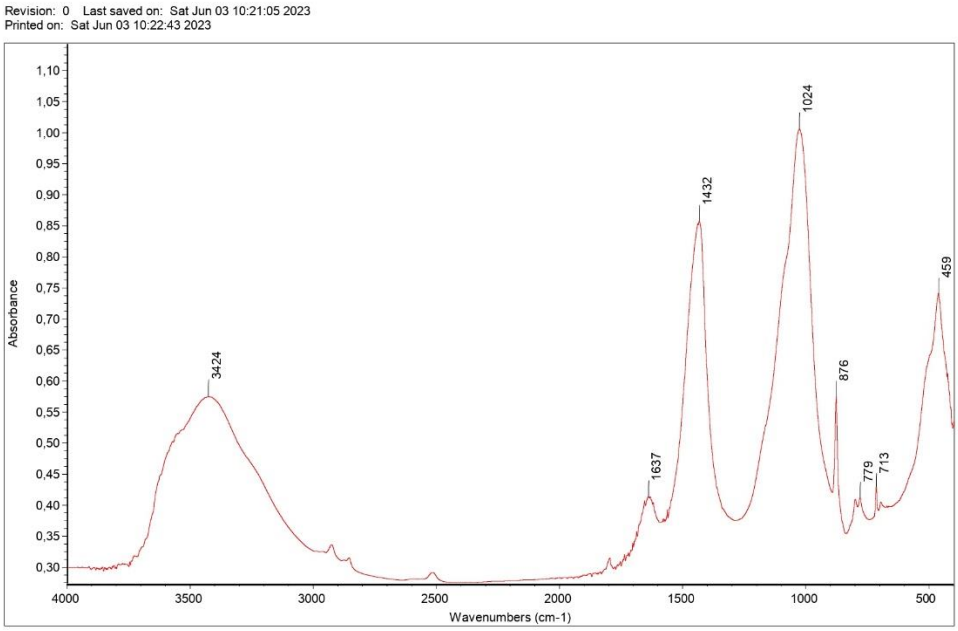

Figure 26. FTIR spectrum from 1003s2 (concrete pier W1003)

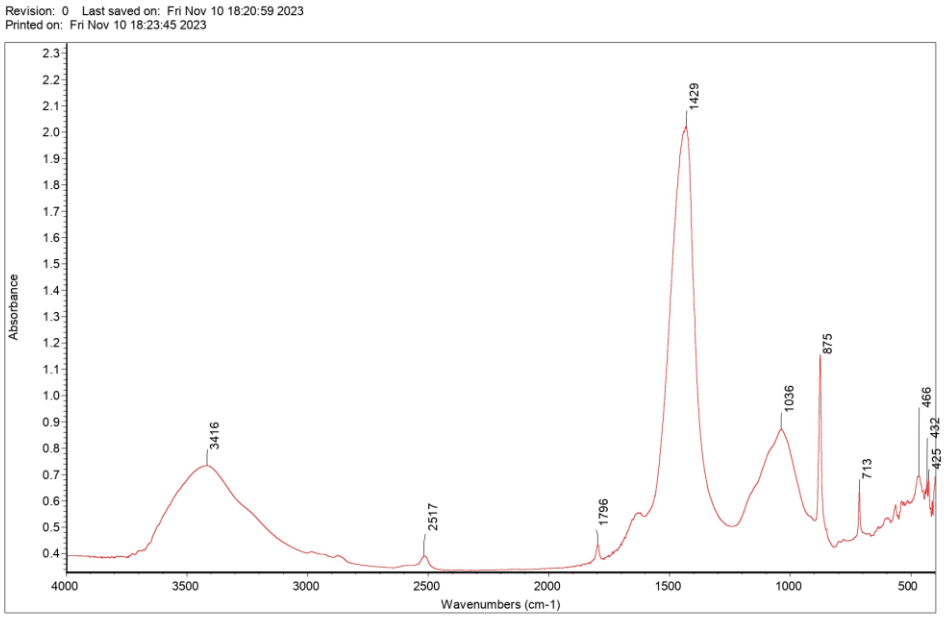

Figure 27. FTIR spectrum from 2006s1

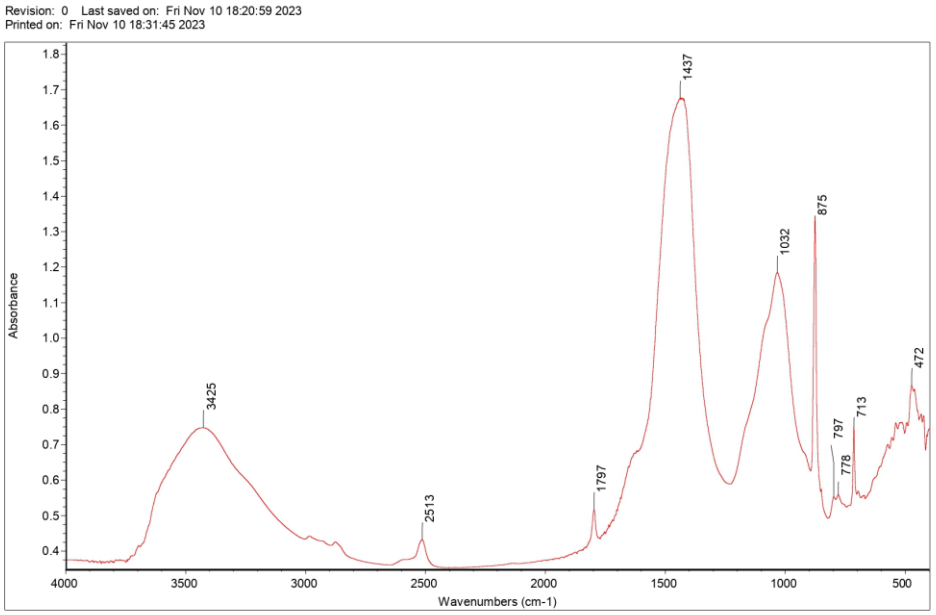

Figure 28. FTIR spectrum from sample 3004

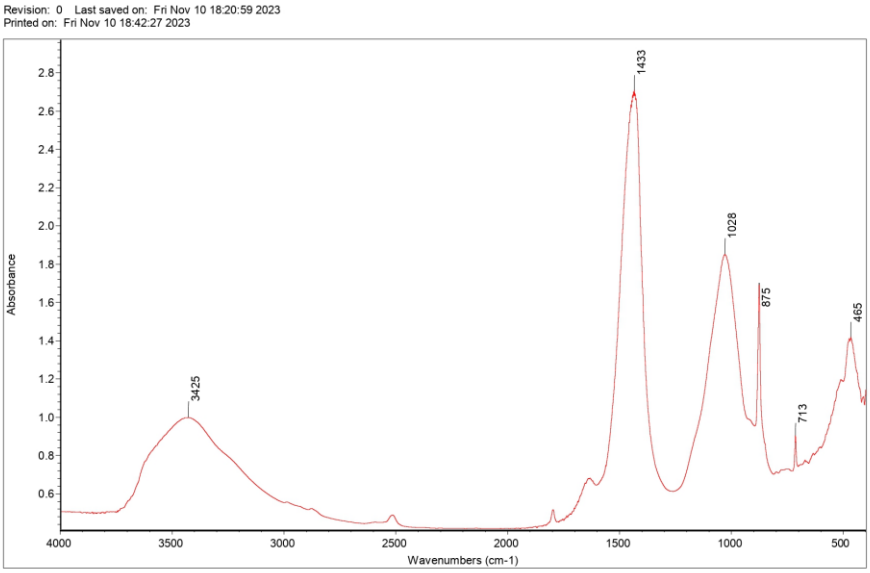

Figure 29. FTIR spectrum from sample 2005.

6.3. XRPD results on bulk samples

The XRPD analysis confirmed the presence of basalt rocks as a main aggregate in the mortars of Tiberias. The main minerals which are associated with basalt rocks are andesine, diopside, nepheline and magnetite. Basalt is a volcanic rocks which comes from the area around Tiberias. Moreover, the presence of hematite in the binders which is an iron oxide is related to the ceramic fragments, since they may contain calcined clays with a relevant occurrence of iron oxide.

The XRPD results showed the occurrence of apatite. Apatite could be related to the ash which has been added to the mortars as an artificial pozzolanic material. The analysis also showed traces of dolomite. Dolomite has a magnesian composition which may be present in the water of the lake, as the Sea of Galilee has a high percentage of salinity. Furthermore, we can assume that the builders of the structures in Myriam's Well beach made use of dolomitic stones for the manufacture of the mortars.

The most significant phase which has been noticed in the mortar samples of Tiberias are the C-A-S-H phases (calcium–alumino-silicate-hydrates). These phases develop because of the reaction between the lime and the aluminosilicate compounds in a water-saturated, highly alkaline environment. The patterns display the typical characteristics of a semi- amorphous material with broad diffraction peaks (Secco M. et al. 2019, p. 227).

Calcite is present in all the samples indicating to us the aerial reaction of the lime when it is set for the construction of the buildings. Lime was the main building material for the mortars in Myriam's Well beach.

6.4. XRPD quantitative analysis

The results of the quantitative analysis are presented in the Tables 2 and 3, whereas the results of the PCA are presented in the figure 1 through the scatterplot (biplot) of the first two principal components (PC1 and PC2), obtained after log-transformation of the quantitative mineralogical data, and representing 61.14% of the whole dataset variance (Secco et al. 2022, p. 5). According to the statistical treatment, the samples were clustered in 4 distinctive groups.

Group 1.

This group is characterized by negative values of PC1 and PC2. The main characteristic of this group is the relevant aerial reaction in the binders. It consists of the mortar samples taken from the walls of the Long Structure 3001, 3002, 3011 (plaster), 2003 (2003_s1), 2001F207, 3004, 3003_FB (fallen blocks which were on top of the pierced ashlar stones) and the piece of plaster found in L327 close to W3010. More specifically, the occurrence in calcite in this group is quite significant, while the presence of phyllosilicate gels (smectite-like) is irrelevant.

Group 2.

This second group is characteristic for a moderate aerial reaction of the respective binders. It consists of values of negative PC2 and positive PC1. It contains the samples 2001, 2001 “Door” (2001_D) 2003_s2, 2004 and 2006. The occurrence of calcite is still important but slighter than the previous group. The presence of phyllosilicate gels in this group remains scarce similar to the first group.

Group 3.

The third group is characterized by positive values of PC2. The reaction of its samples can be described as moderate hydraulic with the development of C-A-S-H phases. In this group, there are samples taken from the W2005, the pavement in the northern part of the W3002 (3002_P), W3005, W3006, W3008 (sewer), W3010. The occurrence of calcite in this group can be described as significant, whereas the amount of phyllosilicate gels is moderate. However, sample 3010 seems to be different regarding its pozzolanic reaction, since its content in phyllosilicate gels is quite little. The mortar samples taken from the sewer 3008 and the pavement from the W3002 can be described as having a high amount of phyllosilicate gels which can be comparable with the last group which is presented below. The samples 3010 and 3008 have a high amount of dolomite compared to the rest of the samples in this group which is related to the use of dolomite mineral during their manufacture.

Group 4

The fourth group has samples taken from the City Wall (1002_A3 and 1002_D) protruding in the lake and the concrete pier (1003) which is underwater. The samples are characterized by an intense hydraulic reaction with the development of the poorly crystalline C-A-S-H and M-A-S-H phases. More specifically, their amount in calcite could be characterized as moderate, while the presence of phyllosilicate gels is

described as high except for the sample 1002_A3 from the City Wall which appears to be moderate. The occurrence of dolomite is noticeable in the samples 1003 (concrete) pier which was underwater. In this case the significant proportion in dolomite fraction could be related to the M-A-S-H phases which have been developed in the binders because of the salinity of the Sea of Galilee.

Outlier 3003_AQ

This sample cannot be identified with one of the groups described above. It can be described as having a high amount of calcite and a scarce occurrence of phyllosilicate gels. On the other hand, it could be characterized by a high amount of apatite (originating probably from ashes of animal remains). Also the occurrence of M-S-H phases in this sample seems to be significant as shown by SEM-EDS analyses.

Sample	1002_A3	1002_D	1003_D	2001	2001_207	2001_D	2003_S1	2003_S2	2004
Amorphou	21.96	24.45	23.19	20.19	30.77	14.90	26.15	18.14	20.37
Ps gel	12.81	23.67	24.47	2.49	1.08	2.29	3.31	3.30	2.40
Ilmenite	0.52	0.18	0.32	0.71	0.74	0.55	0.73	0.49	0.75
Magnetite	0.85	0.95	0.12	0.72	0.43	1.02	0.31	0.76	1.11
Hematite	0.89	0.25	0.41	0.85	0.21	1.27	0.33	0.98	1.32
Forsterite	2.72	0.00	0.00	2.39	0.00	2.03	0.00	2.07	2.00
Diopside	9.86	10.24	5.52	11.95	5.46	12.19	3.49	10.39	13.76
Na-nepheline	2.73	1.59	1.38	4.06	0.33	5.83	1.04	5.17	6.65
Andesine	10.74	13.45	10.21	11.79	2.82	7.96	4.05	8.66	11.90
Quartz	11.58	7.74	9.51	1.95	0.62	1.58	2.28	2.16	2.43
Apatite	0.42	0.00	0.00	1.46	0.00	1.93	0.00	1.53	1.72
Dolomite	0.41	0.64	2.22	0.40	4.24	0.31	0.00	1.00	0.65
Calcite	24.52	16.85	22.66	40.74	46.60	48.15	57.14	45.36	34.97

21.72	22.24	21.62	17.74	31.59	28.97	33.59	15.62	20.14	23.84	14.16	18.58	17.54	22.85
8.36	1.19	4.83	2.31	20.59	3.39	2.95	7.42	10.45	11.79	18.08	3.58	4.18	1.06
0.42	0.47	0.46	0.44	0.28	1.20	0.64	0.61	0.94	0.37	0.47	0.66	0.62	0.52
0.95	0.98	0.87	0.57	0.33	0.82	0.27	0.00	0.70	0.70	0.00	0.90	1.23	0.95
0.32	1.25	0.14	0.46	0.14	0.46	0.09	0.38	0.48	0.67	0.00	0.68	0.45	0.47
0.00	1.45	0.00	0.46	0.00	0.94	0.00	0.00	1.59	0.74	0.00	0.54	0.00	0.00
7.49	9.39	5.49	5.13	3.14	6.02	3.57	0.00	9.43	6.62	0.00	8.45	5.60	2.26
1.48	5.52	0.96	1.26	0.00	1.57	0.00	0.00	0.63	1.85	0.00	2.03	1.45	1.40
5.82	6.90	5.02	5.77	1.14	4.23	1.73	2.07	17.74	5.85	2.06	11.51	7.09	4.06
1.98	2.63	1.71	1.32	2.12	2.84	1.37	2.41	2.93	2.14	4.30	3.27	3.66	3.89
0.00	1.33	0.00	0.00	0.73	4.67	1.05	0.00	0.00	0.00	0.00	0.00	0.00	1.14
1.94	0.52	1.90	4.48	0.00	0.94	0.00	0.00	0.36	1.10	8.36	2.99	3.03	1.66
49.52	45.70	57.01	60.06	38.72	43.97	54.75	70.93	34.26	41.30	48.66	46.81	55.17	59.74
2005	**2006**	**3001**	**3002**	**3002_P**	**3003_AQ**	**3003_FB**	**3004**	**3005**	**3006**	**3008**	**3010**	**3011**	**L327**

Table 3. Mineralogical quantitative phase analysis of the analyzed bulk samples, obtained by full profile fitting of the experimental XRPD patterns according to the Rietveld method

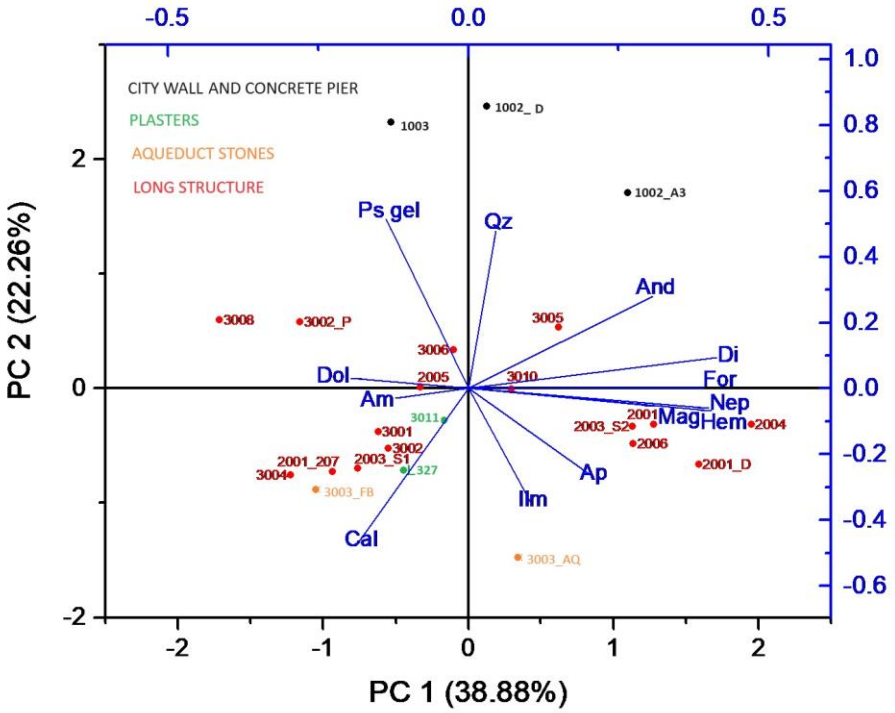

Figure 30. Biblot of the PCA (principal component analysis performed on the mineralogical quantitative data obtained from the analyzed bulk samples: the first two components have been plotted representing 61.14% of the total variance. Abbreviations: Cal = calcite, Dol = dolomite, And = andesine, Di = diopside, For = forsterite, Nep = Na-Nepheline, Mag = magnetite, Hem = hematite, Ap = apatite, Ilm = ilmenite, Qz = quartz, Am = amorphus, Ps gel = phyllosilicate gel. Colors: Red = mortars from Long Structure, Black = mortars from the City Wall and the concrete pier, Orange = mortars from aqueduct stones, Green = plasters.

6.5. Petrographic characterization of the groups

After the statistical treatment by PCA of the XRPD quantitative data, I performed a petrographic study on each sample with the use of a petrographic section.

The main aggregates which have been observed under the microscope are basalt aggregates and volcanic clasts. The volcanic clasts contain feldspars, olivine, and pyroxenes. Ceramic fragments (cocciopesto) have also been noticed which have been added as pozzolanic material. Other aggregates which have been seen are pyroxenes, quartzites and carbonate rocks. Finally, I observed the presence of inorganic residues of organic matter.

The basalt aggregates and the volcanic clasts are well rounded with high sphericity which means that they had been through a sieving process before their addition to the binder. The aggregates are well sorted in most of the thin sections.

The binder matrix can be characterized as amorphous and heterogeneous in most of the cases. Some samples may show a micritic calcareous matrix as well.

The microscopic characteristics of each group of mortars is described here, whereas there are some differences within groups.

Group 1

This group can be subdivided into different subgroups, since the petrographic study has shown different results for some samples. The first subgroup contains four samples (3001, 3002, 3011, L327). These samples correspond to the walls w3001, w3002 and w3001 and another one is piece of plaster found in L327. The thin sections of this group are rich in basalt aggregates and volcanic clast. However, the lack of ceramic fragments is evident. Quartzites and carbonates are also detectable in little quantities. The basalt and the volcanic clasts can be described as subrounded with high sphericity in many cases. The aggregates are poorly sorted in the matrix.

The color of the matrix varies from dark brownish to grey and whitish. It is heterogeneous with an amorphous appearance. The presence of lumps is medium, and they are mostly showing the textural features of underburnt calcite. The particle size for the basalt and the volcanic clasts of that group is 7000 – 300 μm (fine gravel to medium sand). The quartzite aggregate varies from 1000 μm to 100 μm (very coarse sand to very fine sand). Ceramic fragments are scarce, and their size is around 600 μm (coarse sand).

The second subgroup includes the mortar samples 3003 FB (the fallen blocks which were on the top of the aqueduct stones), 2003_s1, and 2001 F207 (the step in front of the “door” in w2001) which are mainly fat binders in the aliquots of basalt aggregates is medium to high. Ceramic aggregates are present but scarce. There are a few isolated clinopyroxenes minerals used as aggregates. Quartz and carbonate rocks as aggregates are low.

Macroscopically, the matrix color appears to be whitish. Under the microscope, the binder matrix can be described as whitish greyish to brown. It is micritic and heterogeneous. The particle size for the basalt aggregates can vary from 6000 to 350 μm (fine gravel to medium sand). Carbonate rocks have a particle size of 6700-150 (fine gravel to very fine sand). Clinopyroxene minerals vary from 800 to 50 μm (coarse sand-silt). Charcoal and inorganic tissues of biogenic origin are common in this group which shows to us that ash has been added to the binders as a pozzolanic materials. Small particles of ash are visible in the binder matrix.

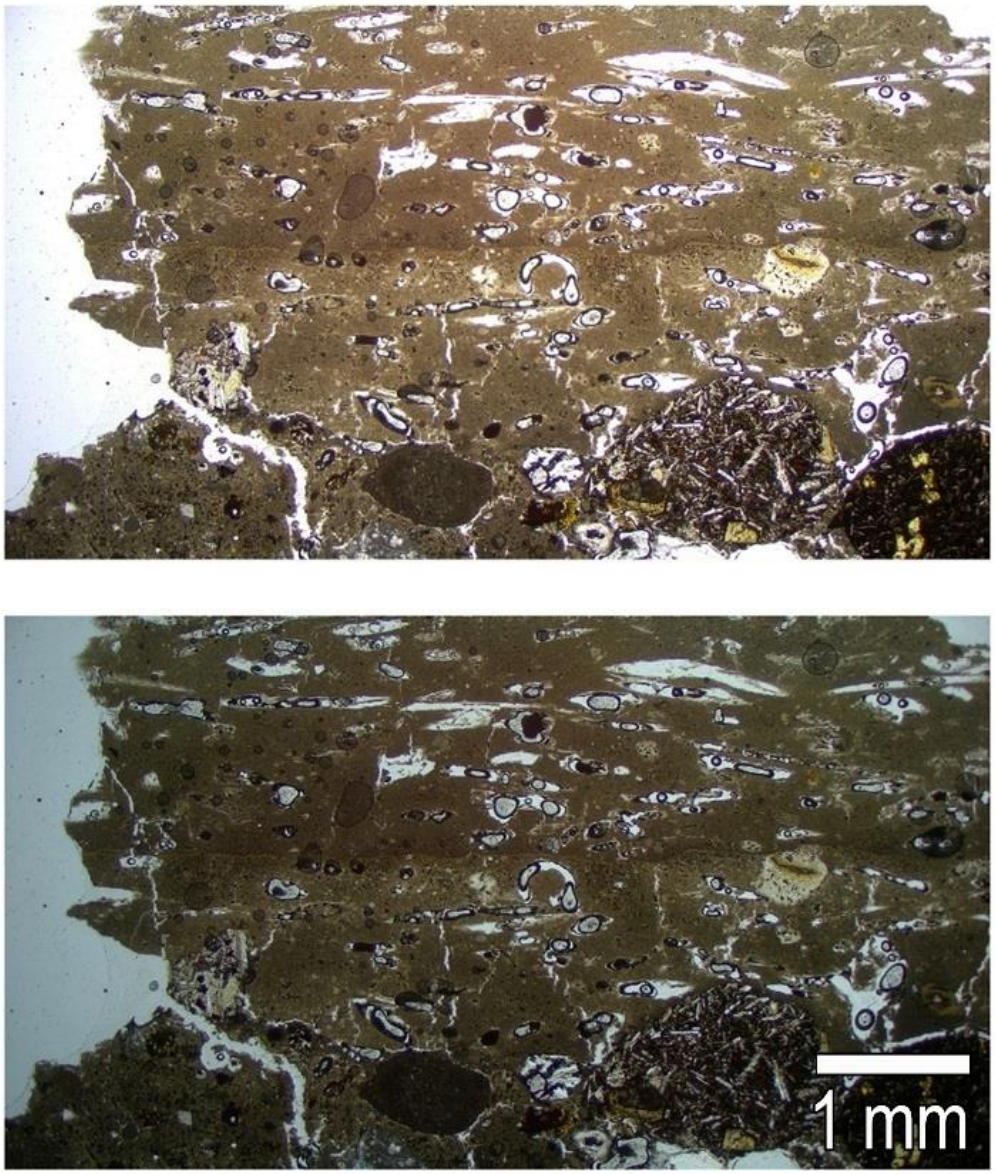

Figure 31. Sample L327 (Plaster). PPL above and XPL below. Different layers of plastering (First one brown, second one light brown). Magnification is 1.6X.

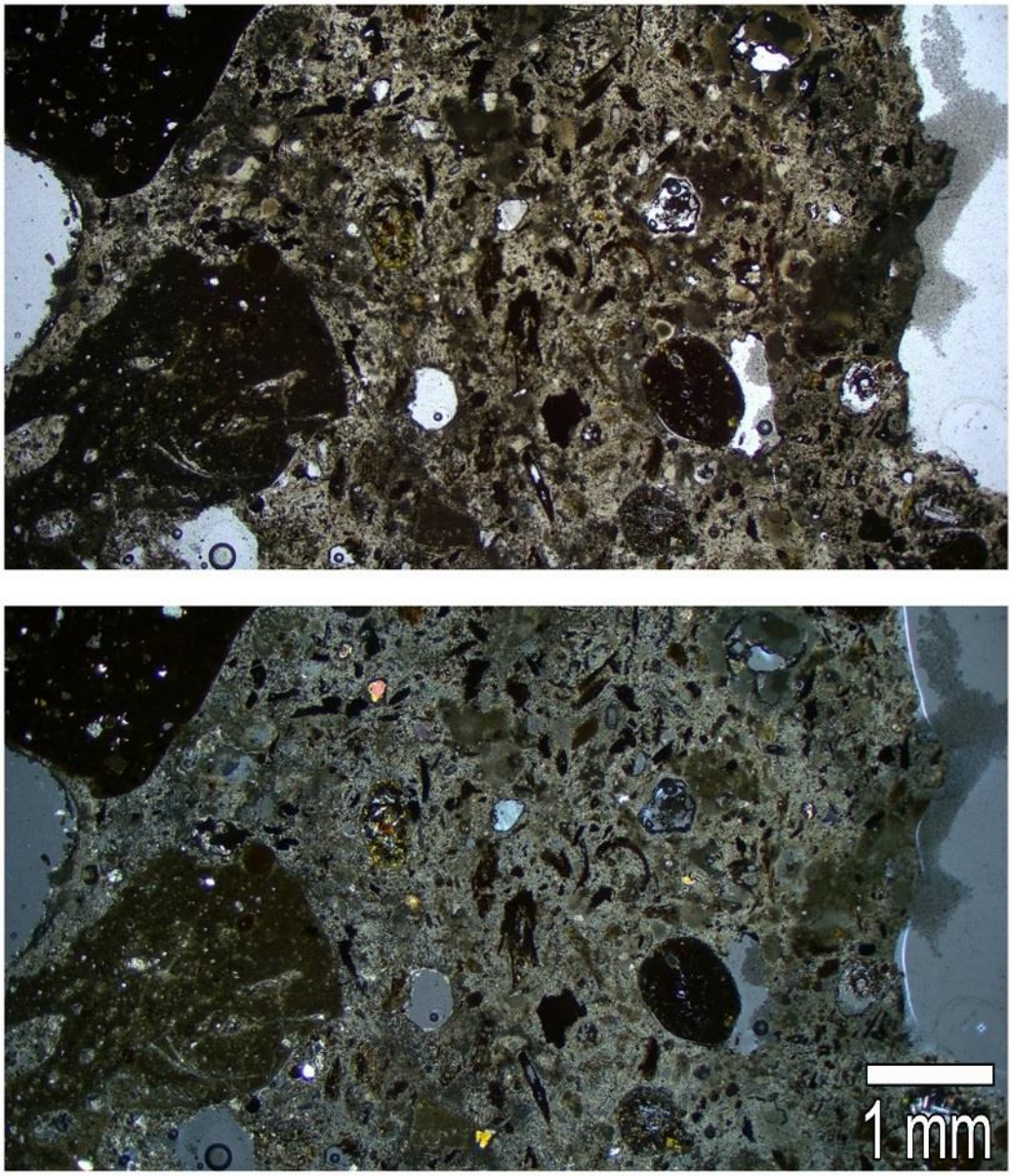

Figure 32. Sample 3003_FB. PPL above XPL below. Charcoal and ash particles. Magnification is 1.6X.

Group 2

The first group contains the samples taken from the wall 2001, 2004, 2006 and 2003 (samples 2001, 2001 door, 2004, 2006 and 2003_s2). Their main composition is basalt aggregates and clasts. Carbonate rocks and quartzites are also detectable in smaller quantities. The pozzolanic material which has been used for the manufacture of these samples is ceramic fragments. The aggregates of this group can be characterized as subrounded-subangular. The basalt aggregates and clasts have high sphericity, whereas the ceramic fragments have low sphericity and are subangular in most of the cases.

The binder matrix is brownish and amorphous. It is homogeneous in all the areas of the samples. It seems to be a fat binder and only the binder of the sample 2001 door appears to be leaner. The number of lumps is low with a texture typical for underburnt calcite. The particle size for the volcanic clasts and the basalt aggregates varies from 10000 μm to 250 μm (medium gravel to fine sand). The size particle for the ceramic fragments varies from 3500 to 50 μm (very fine gravel to silt). Quartzite aggregates vary from 100 to 600 μm (coarse sand to very fine sand). Carbonate rocks which are scarce have a size of 1850-250 μm (very coarse sand to fine sand). The aggregates can be described as well-sorted.

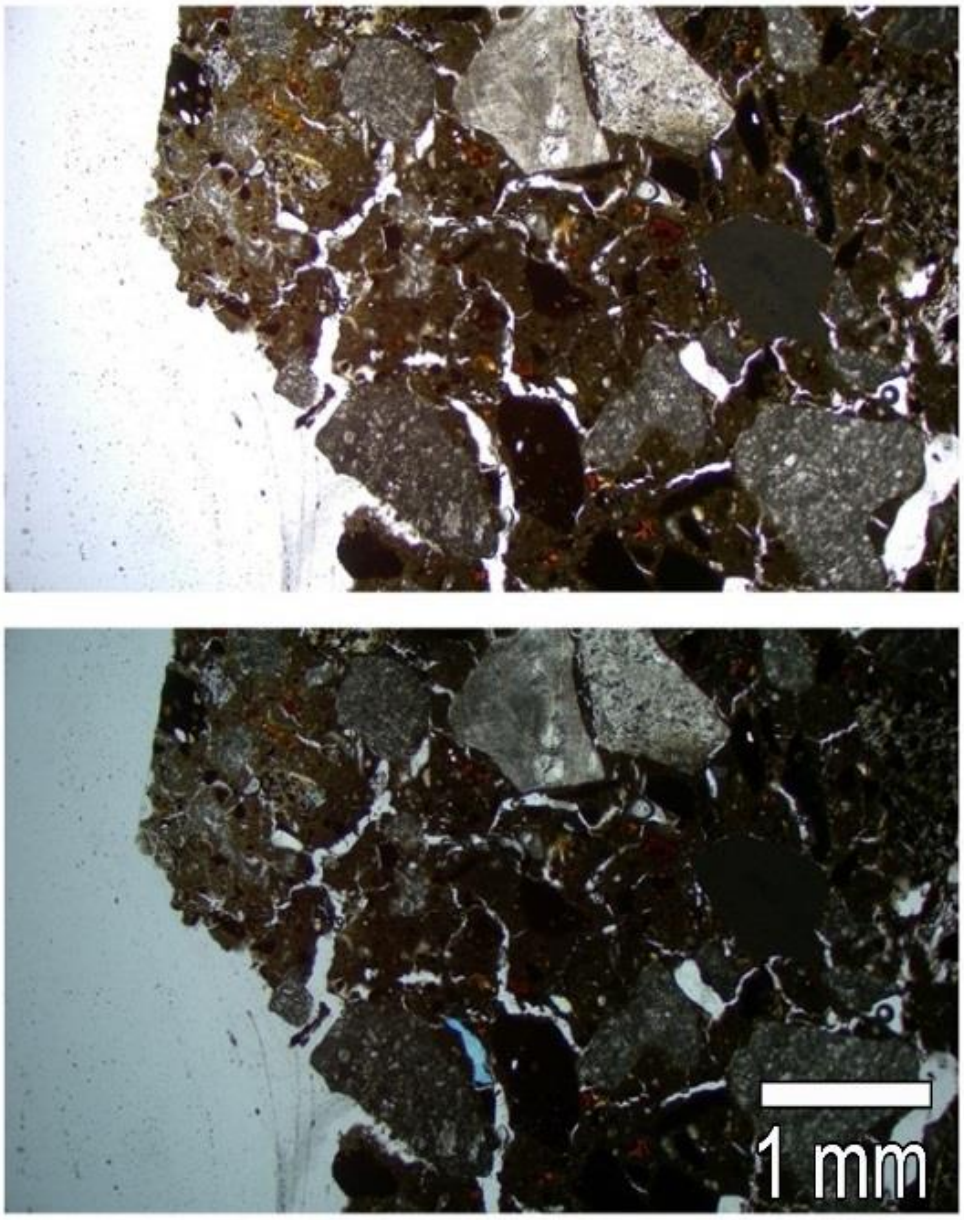

Figure 33. Sample 2001. PPL above, XPL below. Basalt aggregates and brownish amorphous matrix. Magnification is 1.6X.

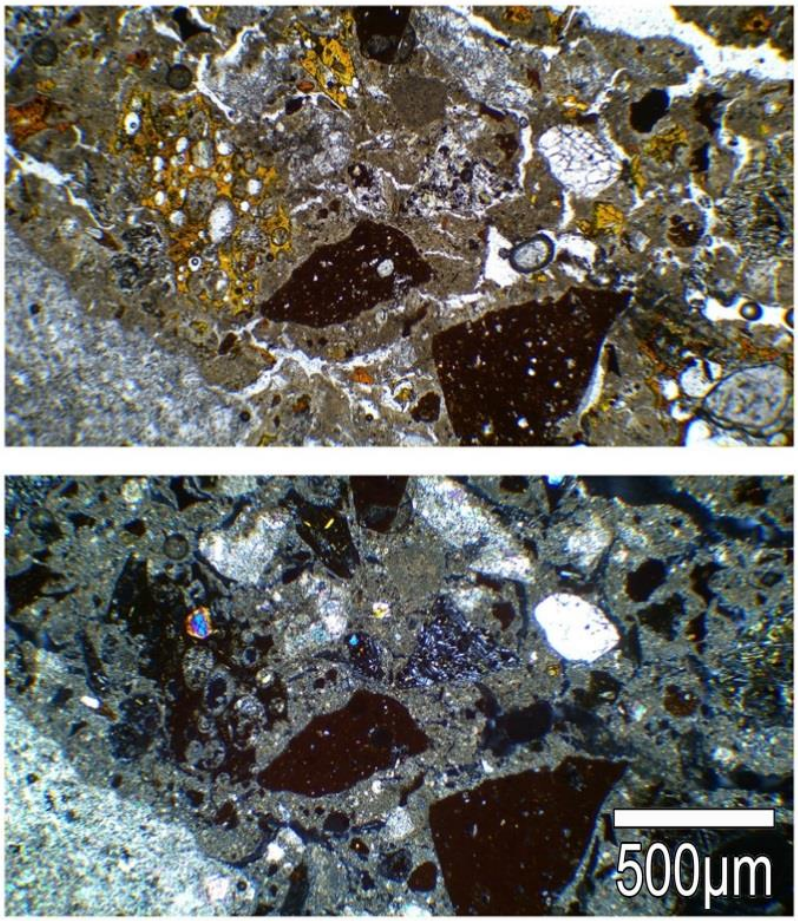

Figure 34. Sample 2006. PPL and XPL images. Ceramic fragments (cocciopesto). Magnification is 4X.

Group 3

There are four samples in the fourth group which are 2005, 3005, 3010 and 3008. They are all fat binders. The sample 3008 seems microscopically and macroscopically quite different from the rest of the samples in this group, so it should consist of a separate subgroup. The main aggregate composition of the samples in this group is basalt rocks and clasts. Their size varies from 16000 μm to 100 μm (medium gravel-very fine sand). Quartz aggregates are also present in the aggregate fraction of this group in a medium quantity. Their size could vary from 500μm to 100μm (medium sand – very fine sand). Pyroxene minerals which have been added as aggregates are present in average quantities. Their size is from 800μm to 100μm (coarse sand to very fine sand). Carbonate rocks as aggregates appear to be present in little quantity. The size of this type of aggregate is 6.750-200 μm (fine gravel to fine sand). The aggregates can be described as subangular – subrounded with high sphericity, especially for the basalt clasts. Ceramic fragments are not detectable in this group. Only some skeletal tissues and vegetal tissues are present in the samples 2005 and 3005.

The binder matrix appears to be amorphous and heterogeneous, while only samples 2005 and 3008 have a micritic texture in the matrix. The color can vary from dark brown to brown and grey in some cases. The number of lumps is low and they are showing the typical feature of underburnt calcite. The amount of voids is medium and are mostly vughs and channels. Only the sample 2005 has a higher number of vughs than the rest of the samples.

The sample 3008 was taken from the wall which constitute the sewer (w3008 and w3009) in the southern end of the "Long Structure". It should be separated from the rest of the samples in the third group because of its appearance both macroscopically and microscopically. It contains a high aliquots of quartzites and carbonate aggregates and scarce pyroxenes and basalt rocks. The particle size of the aggregates varies from 500 to 60 μm (medium sand to silt). Tissues of biogenic origin have also been detected which shows to us that there was the addition of ash to the binder. The binder is mainly composed of anthropogenic calcite mixed with clay as the macroscopic view showed to us. The matrix can be characterized as micritic and homogeneous. Lumps are not present and the number of voids (vughs and channels) is low.

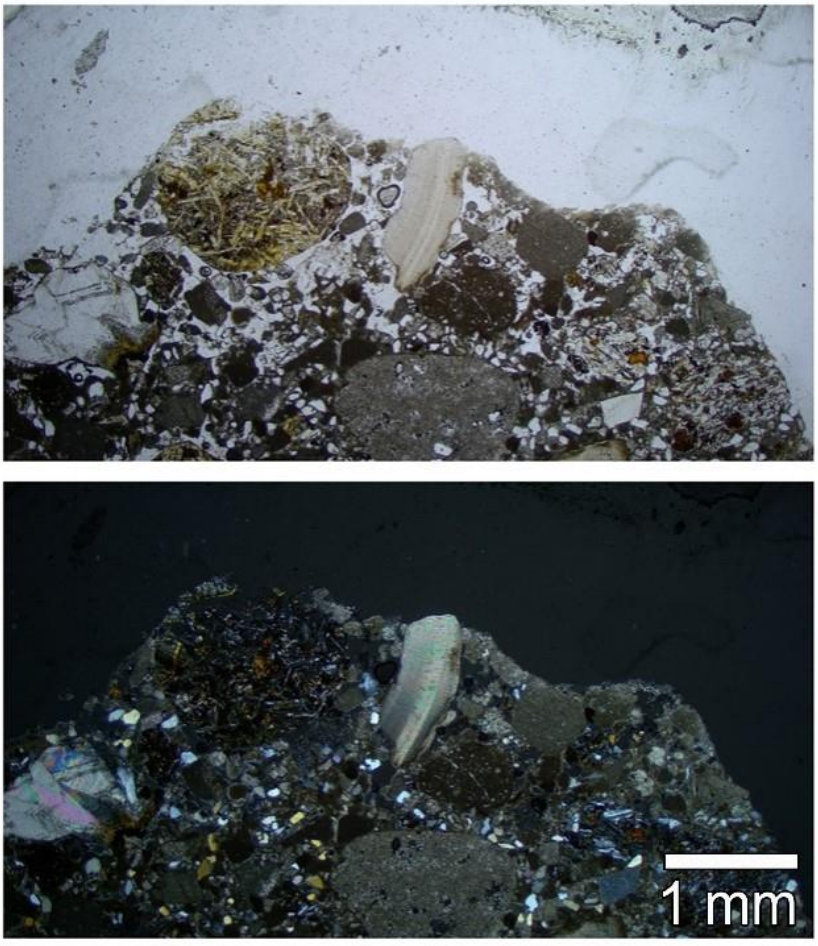

Figure 35. Sample 3005. PPL above and XPL below. Skeletal tissue and basalt clasts. Magnification is 1.6X.

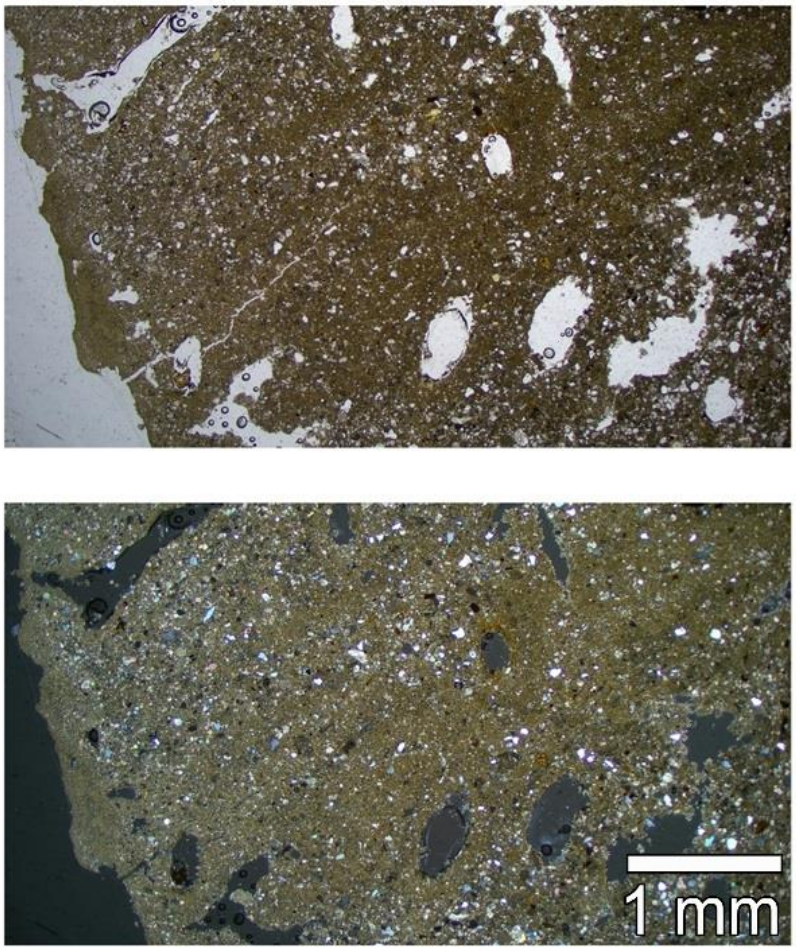

Figure 36. Sample 3008 (sewer). PPL above XPL below. Quartzite aggregates and micritic matrix. Magnification in 1.6X.

Group 4

The fourth group is composed of mostly lean binders. This group contains the samples 1003 (from the concrete blocks in front of the City Wall), 1002_D (concrete section in front of the city wall), 1002_A3 (part of the city wall). It is composed of basalt aggregates and clasts like the previous thin sections. The number of ceramics in this group can be described as medium to high. The number of quartz aggregates is higher compared to the rest of the mortar groups. The aggregates can be characterized as subangular and subrounded with high sphericity. They are also well sorted. The number of voids is not high, whereas there are some packing voids like the sample 1002 D and 1002 A3.

The matrix of these binders could be described as micritic and heterogenous. There is a variation in the color from whitish and light brown to dark brown. In some areas of the thin sections, it can appear an amorphous matrix. The particle size of the basalt aggregate varies from 7500 to 150 μm (fine gravel to coarse sand). Quartz aggregates have a smaller size which is from 900 to 100 μm (coarse sand – fine sand). The ceramic fragments vary from 1200 to 150 μm (very coarse sand – fine sand).

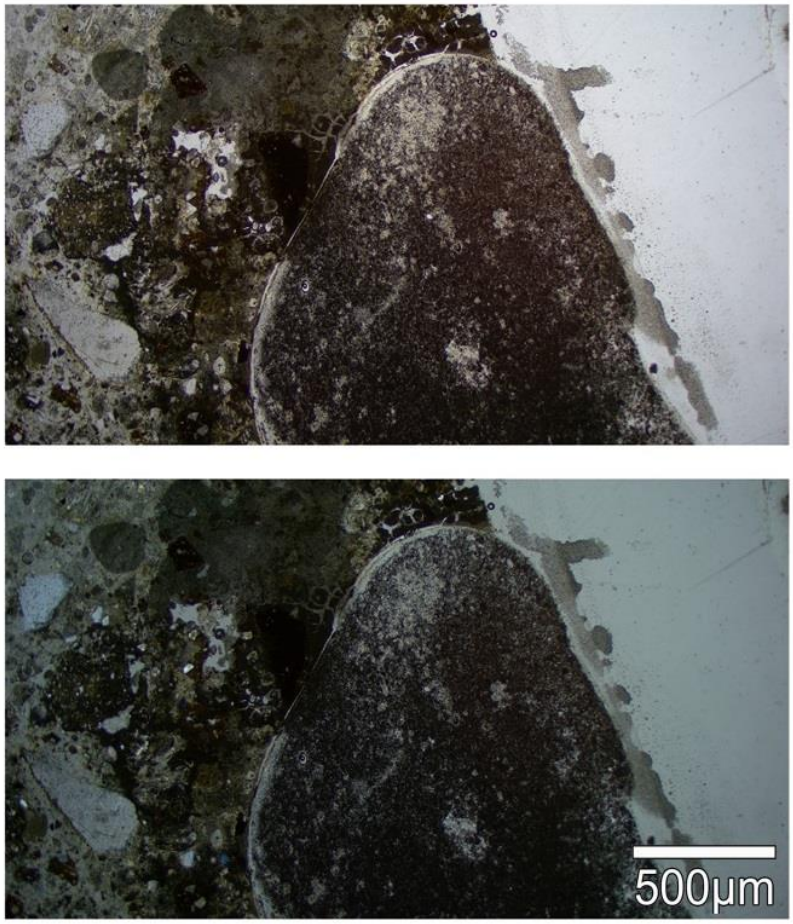

Figure 37. Sample 1002_D. PPL above, XPL below. Basalt aggregate. Magnification is 4X.

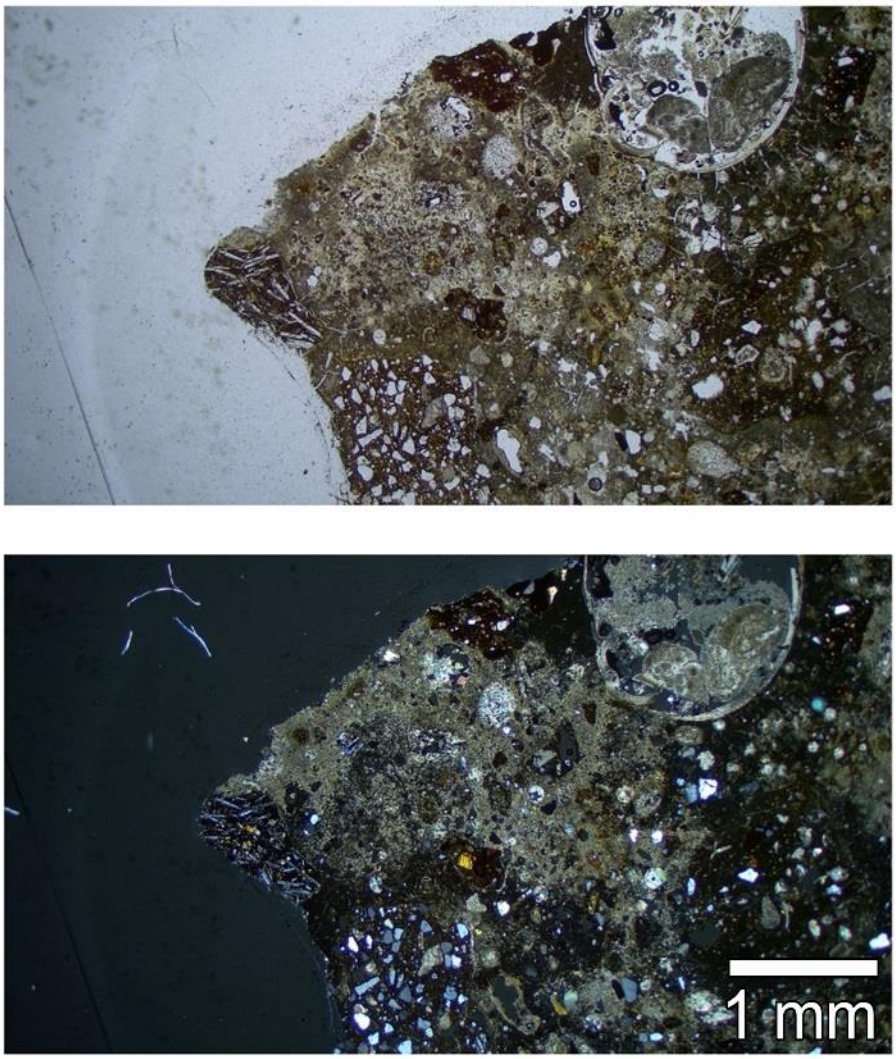

Figure 38. Sample 1003 (concrete pier). PPL above XPL below. Micritic matrix and basalt clasts. Magnification 1.6X

Outlier 3003_AQ

As it was written before this sample consists of an outlier. It is a lean binder, extremely rich in aggregates. Its main composition is basalt rocks and clasts as aggregates. Their size varies from 5000 μm to 300 μm (fine gravel to medium sand). It also includes a high amount of carbonate rocks whose size is from 3000 μm to 500 μm (very fine gravel to medium sand). The number is quartz and pyroxene rocks added as aggregates is little. Their size can vary from 500 μm to 150 μm (medium sand–fine sand). Ceramic fragments are not detected. Shell fragments can be observed, added possibly as aggregates. Biological tissues were noticed as well. The aggregates can be described as subrounded-subangular with high sphericity. They are well sorted in the binder. The binder matrix can be characterized as micritic and heterogeneous with a brownish color. Lumps are absent and the amount of voids is low.

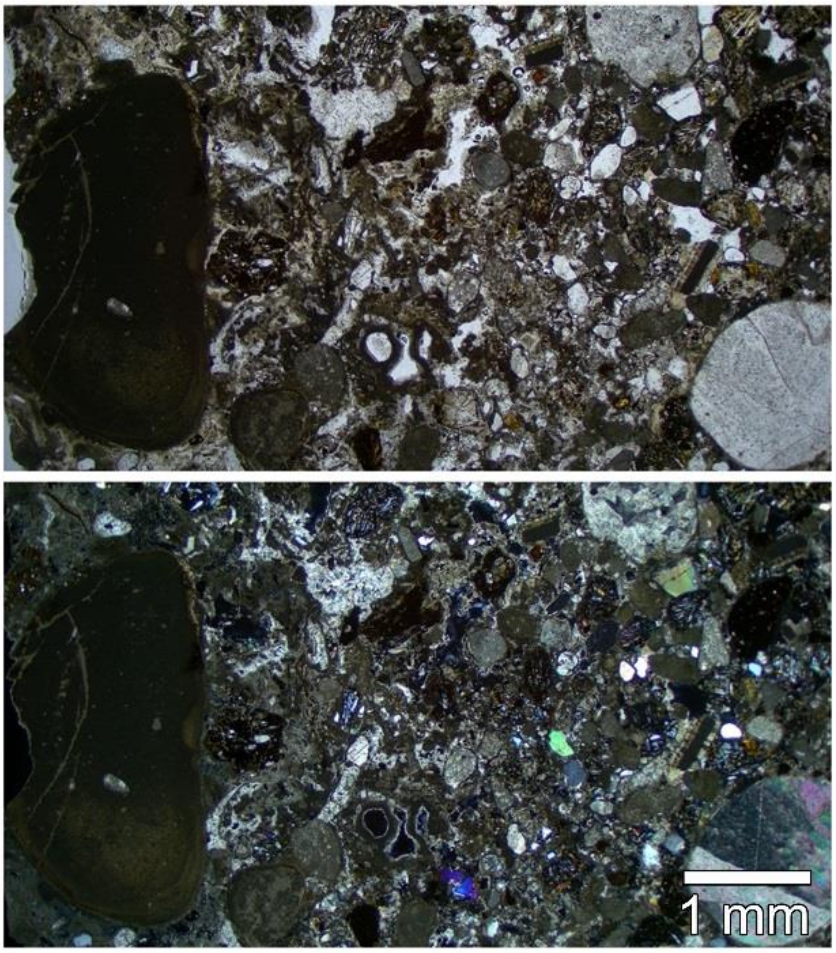

Figure 39. Sample 3003_AQ. PPL above, XPL below. Basalt and quartzite aggregates. Magnification 1.6X.

6.6. SEM-EDS results

The main composition of the binder matrix is Ca which shows to us that the binders were made with the use of pure calcic lime. Other elements which were found in the matrix are Si, Al and Mg. Si and Al correspond to the poorly crystalline C-A-S-H phases which develop due to the reaction between the lime and the aluminosilicate compounds in a saturated alkaline environment. The presence of Mg is associated with the lake environment. The sea of Galilee has a high percentage of salinity. Mg can be also related to the use of dolomitic stones as aggregates in the binders. The presence of Mg gives rise to the formation of the gel-like M-A-S-H in the binder matrix. Small quantities of Na, K, Cl and Ti are also present. SEM analysis has showed the occurrence of small quantities of P which can correspond to the ash which was added to the mortars as a pozzolanic material.

As previously done for the other analytical techniques, I separated the samples tested by SEM in different groups according to their elemental composition. Some of the groups have the same samples of the groups defined by PCA analysis.

Group 1

The first group includes the samples 2003s1, 3001, 3002, 2001 F207, 3011 and 3003_FB, which are located in the south of the Long Structure, as well as the plaster found in L327. These samples are characterized by relevant aliquots of Ca in the matrix and by the abundance in Si and Al. It appears that the pozzolanic reaction and the occurrence of C-A-S-H phases are intense. The samples 3011 and L327 contain more important amount in Ca and have small quantity of Si and Al which can be related to the prevalence of the aerial reaction, since these mortars did come in direct contact with the lake environment.

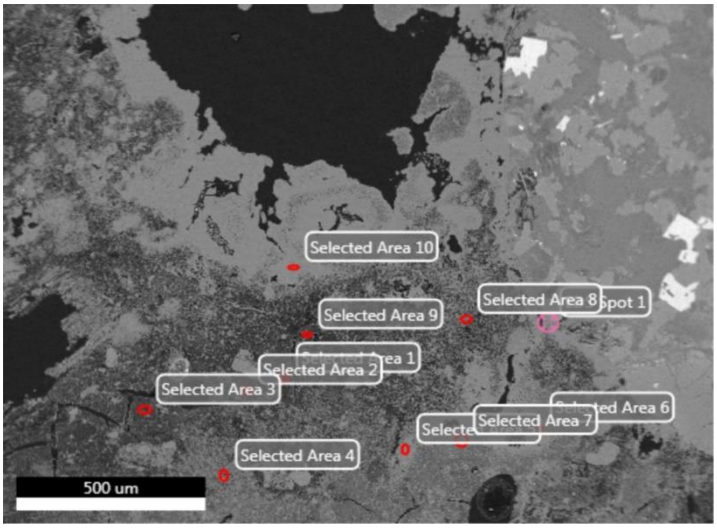

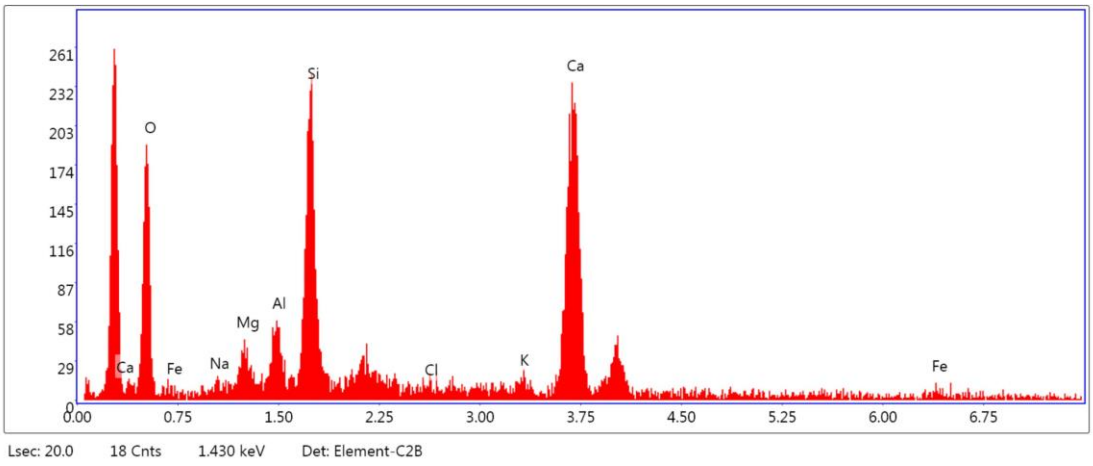

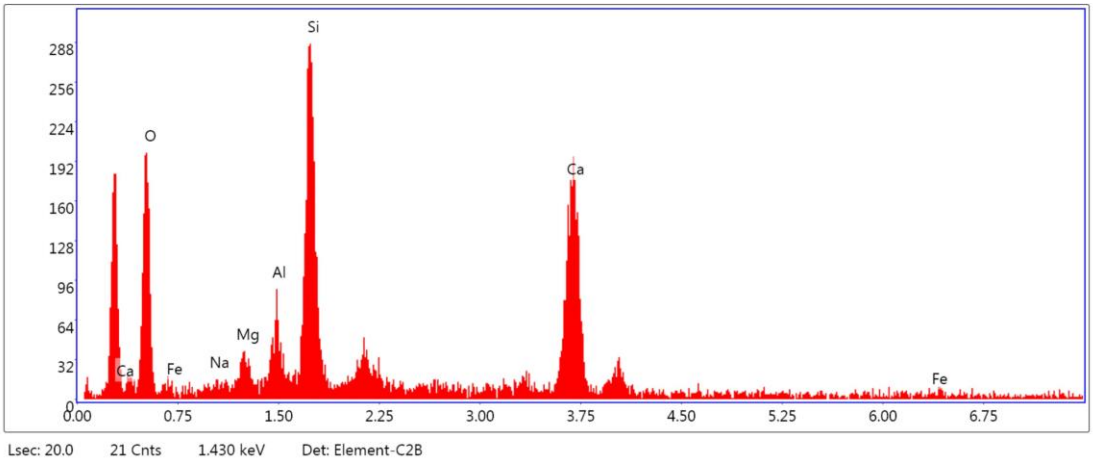

Figure 40. Sample 3001. SEM-EDS image and spectrum from Selected Area 3 and 9.

Group 2

The second group consists of the sample which come from the walls 2001, 2004, 2006, 2003 s2. This group contains samples with high aliquots of Si and Al in the matrix which are indicative for the formation C-A-S-H. However, there are also Mg aliquots. Therefore, we cannot exclude the precipitation of M-A-S-H phases. The amount of Ca remains important. Another element which has been detected in the binder matrices of that group is P. The presence of P can be related to phosphate minerals, like apatite, likely deriving from animal ashes which have been mixed with the binders.

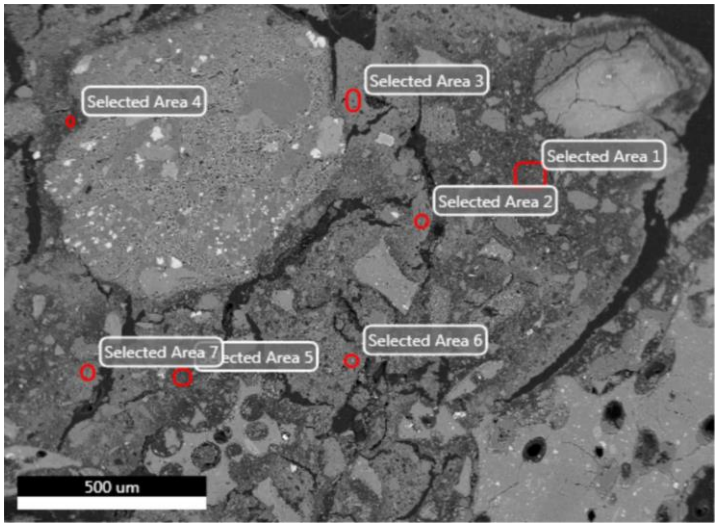

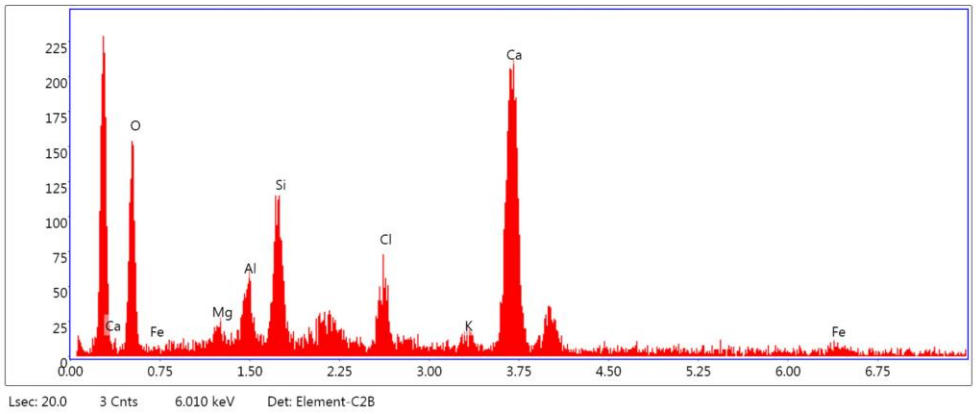

Figure 41. Sample 2006. SEM-EDS image and spectrum from the reaction rim in selected area 4.

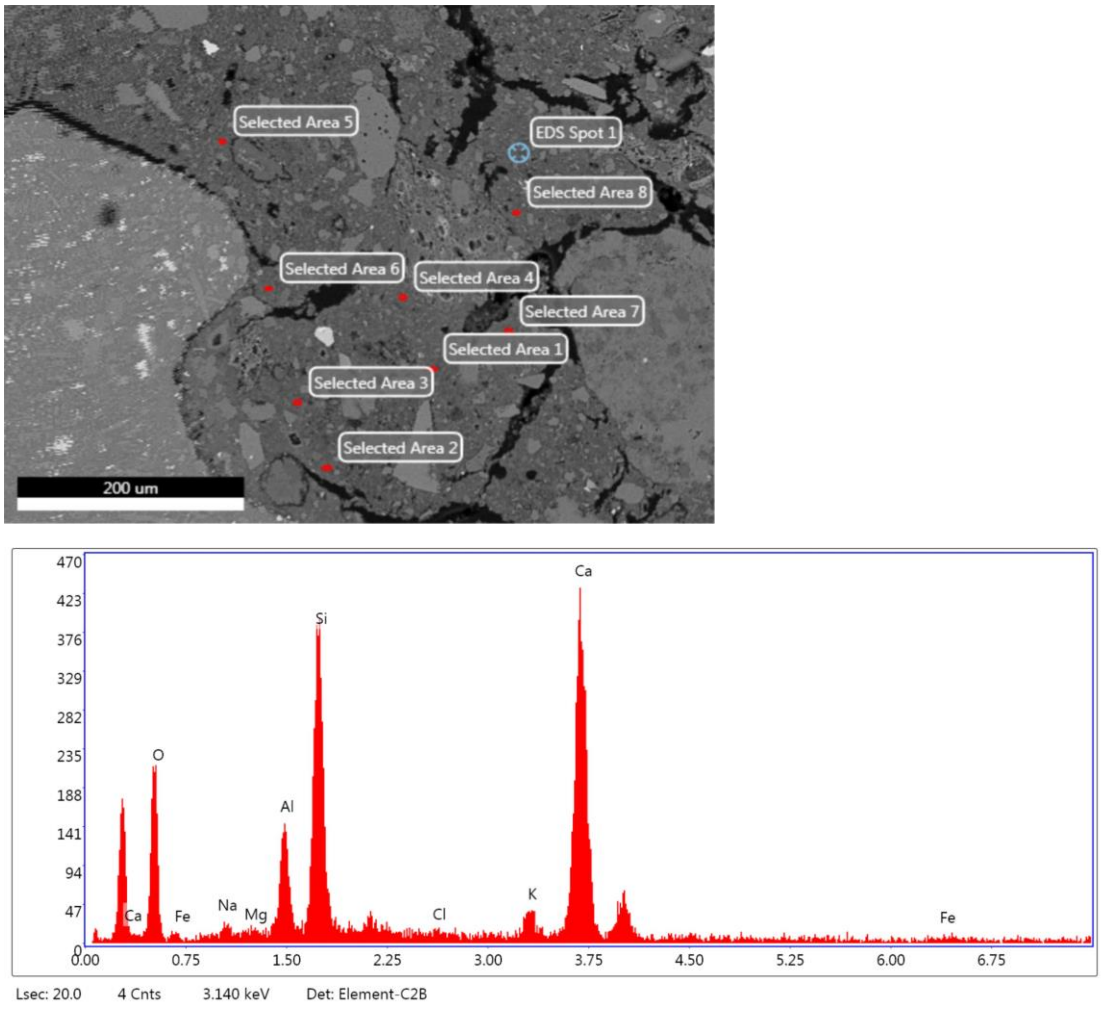

Figure 42. Sample 2004. SEM-EDS image and spectrum from the selected area 4.

Group 3

This group consists of the samples 2005, 3005, 3010 and 3008 (sewer). Samples 2005, 3005 and 3008 contain important quantities of Si, Al and Mg which can be

associated with the formation of paracrystalline M-A-S-H and the C-A-S-H phases. Ca aliquots are significant but less abundant. Sample 3010 which was taken from an inner wall of the Long Structure is characterized by large amount of Ca and little Si and Al suggesting the occurrence of an aerial reaction in the binder of this sample. The occurrence of P can be detected which can be related to the mineral apatite derived from animal ashes.

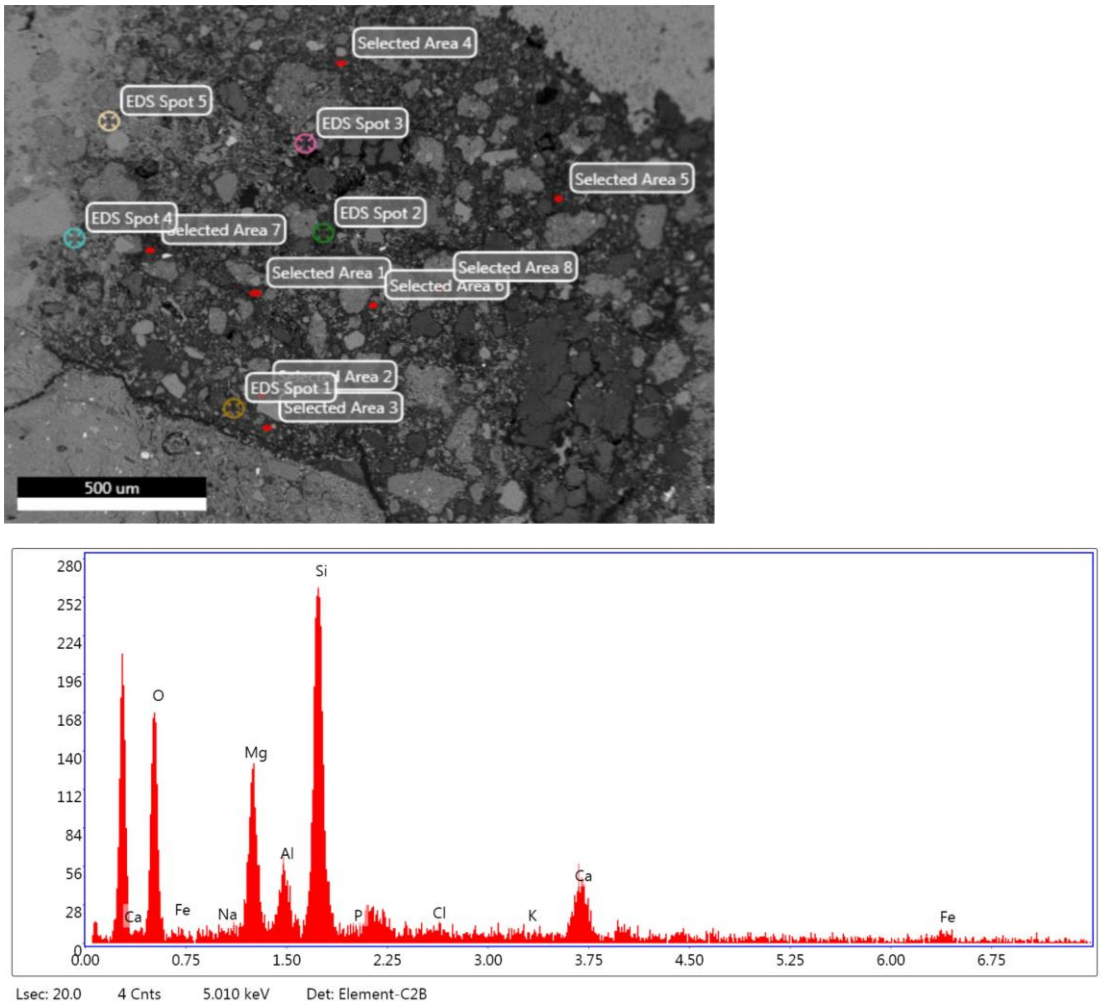

Figure 43. Sample 3005. SEM-EDS image and spectrum from selected area 1

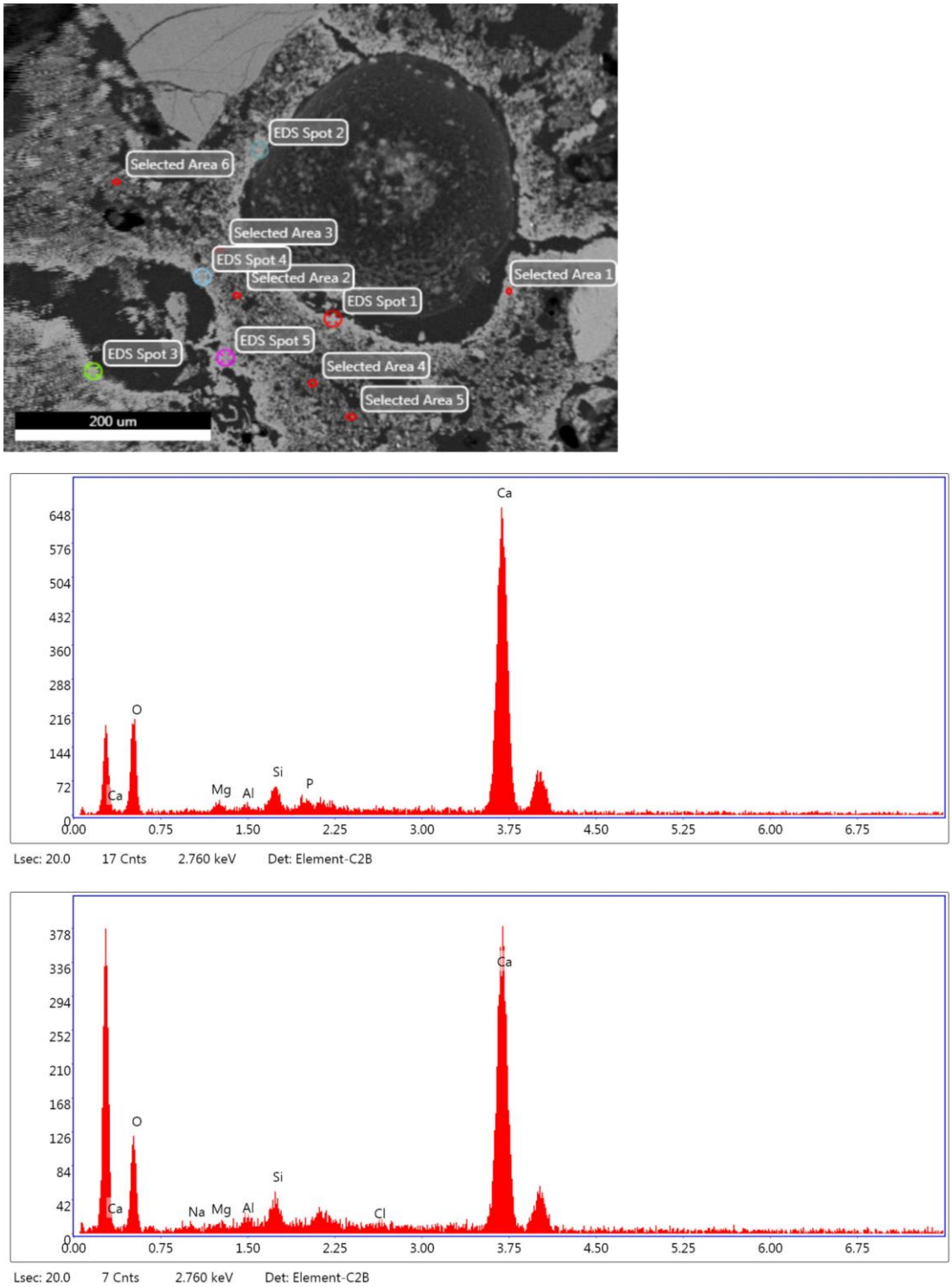

Figure 44. Sample 3010. SEM-EDS image and spectra from selected areas 1 and 2

Group 4

The first group includes the samples which come from the walls 1002 A3, 1002 D (basalt wall from the extension of the city wall), 1003 (concrete pier). In this group, we can notice the presence of large quantities of Si, Al, Mg and Ca, indicative to the occurrence of poorly crystalline C-A-S-H and the AFm phases, such as hydrocalumite

and hydrotalcite. The presence of Mg may correspond to the development of the gel-like M-A-S-H in the binder matrix. The presence of Mg is detected in the Sea of Galilee which is a lake with a high ratio of salinity. The City Wall and the concrete pier are located very close to the lake level and come in touch with the water. The reaction rims which surround the aggregates of this group have a composition typical for M-A-S-H and C-A-S-H phases.

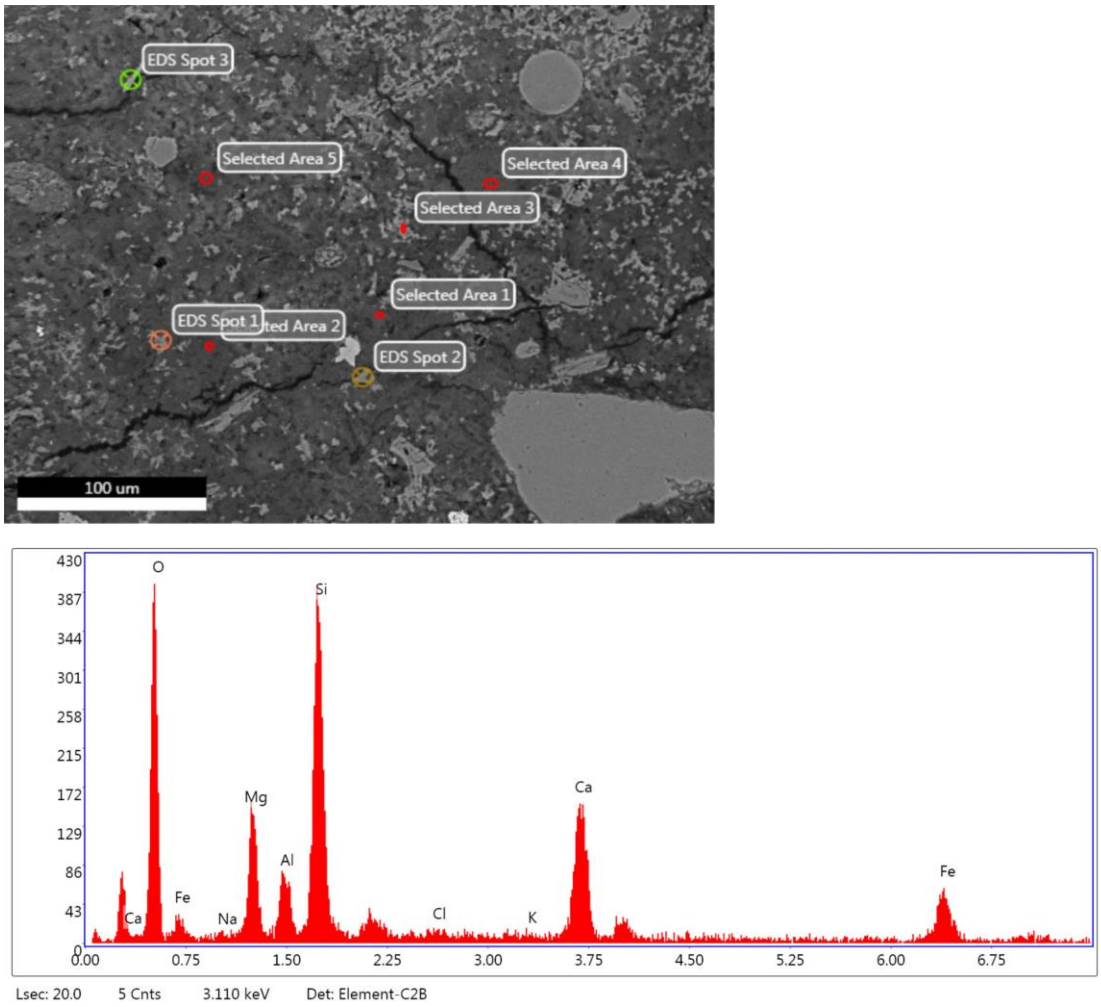

Figure 45. Sample 1003. SEM-EDS image and spectrum from selected area 1.

Outlier 3003_AQ

This group has only one sample which come from the mortars of the aqueducts stones (3003 Aq). This mortar is special because of the high amount of Mg. This mortar has probably a magnesian nature making unique among the rest of the groups. Ca, Si, and Al are also present in the EDS spectrum. Therefore, C-A-S-H and M-A-S-H have been developed in the binder matrix of mortar 3003_Aq.

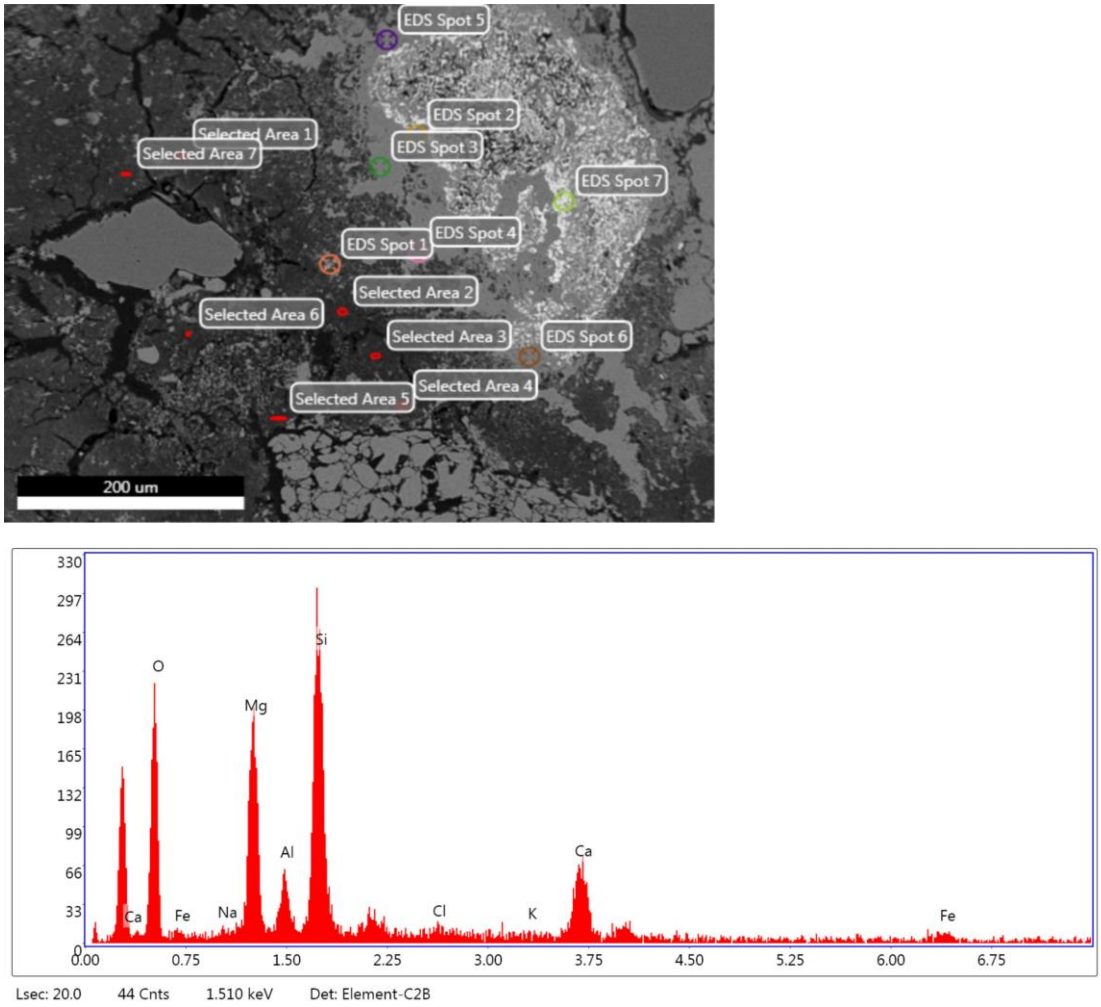

Figure 46. Sample 3003_AQ. SEM-EDS image and spectrum from selected area 2

6.7. Composition of the binder fraction

6.7.1 XRPD on binder fractions

PCA (Principal Component Analysis) was performed on the quantitative results obtained by the XRPD analysis on the binder fractions of the samples. The biplot of the statistical treatment was obtained after log-transformation of the quantitative data, and represents 74.52% of the whole dataset variance. In the biplot, we may clearly observe that the samples are separated in three groups and one outlier.

Group 1

The first group includes samples from the walls 2004, 3011, 2006. They have negative values of PC1 and PC2. These samples have relevant calcite aliquots and a little amount of AFm phases and phyllosilicate gels. As a result, there is an aerial reaction developed in the binders of these samples.

Group 2

This group includes two samples, 1002_A3 and 1003 which come from the City Wall and the concrete pier respectively. They are characterized by positive PC1 values and both positive and negative PC2 values. They can be described as having a large quantity in phyllosilicate gels (smectite like) and a slight aliquots of calcite so that a relevant pozzolanic reaction was developed in the binder fraction of these samples precipitating poorly crystalline C-A-S-H and M-A-S-H phases.

Group 3

The third group is composed of three samples, 2003_s1, 3002 and 3005. They are characterized by mainly positive values PC2 and negative values of PC1. Only 2003_s1 has negative PC2. This group is characterized by an important quantity of AFm phases and phyllosilicate gels which are indicative of relevant pozzolanic reaction processes. However, their hydraulic reaction remains less significant than the one in the second group.

Outlier 3003_AQ

The sample 3003_AQ which came from the concrete of the aqueduct stones from the w3003 is the outlier of the biplot. It has positive values of PC2 and negative values of PC1. This sample has a significant quantity in amophous and AFm phases which can be justified by the development of the C-A-S-H and M-A-S-H phases in the binder fraction.

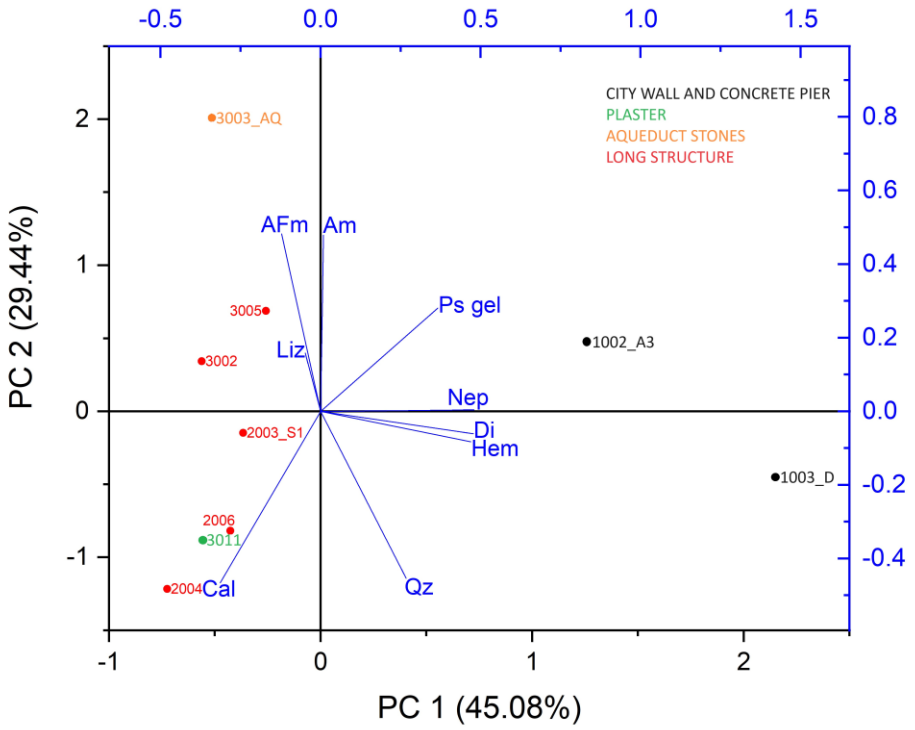

Figure 47. Biblot of the PCA (Principal Component analysis of the mineralogical quantitative data obtained from the analyzed binder fractions: the first two components have been plotted representing 74.52% of the total variance. Abbreviations: Cal = calcite, Di = diopside, Nep = Na-Nepheline, Hem = hematite, Qz = quartz, Am =amorphus, Ps gel = phyllosilicate gel, Liz=Lizardite. Colors: Red = mortars from Long Structure, Black = mortars from the City Wall and the concrete pier, Orange = mortars from aqueduct stones, Green = plasters.

Sample	Calcite	Quartz	Na-nepheline	Diopside	Hematite	AFm phase	Lizardite	Ps gel	Amorphous
1002_A3	2.99	0.42	0.44	2.01	0.27	0.00	0.00	45.10	48.77
1003_D	6.21	1.12	0.44	5.29	0.37	0.00	0.00	49.40	37.17
2003_S1	35.56	0.63	0.00	0.00	0.00	0.00	0.00	13.80	50.01
2004	76.10	0.58	0.00	0.00	0.00	0.00	0.00	2.52	20.80
2006	62.01	0.59	0.00	0.00	0.14	0.00	0.00	0.33	36.93
3002	35.45	0.41	0.00	0.00	0.00	0.56	0.00	6.50	57.08
3003_AQ	5.67	0.00	0.00	0.00	0.00	2.25	0.00	26.44	65.64
3005	19.14	0.08	0.00	0.00	0.00	0.00	0.87	49.00	30.91
3011	61.08	0.64	0.00	0.00	0.00	0.00	0.00	8.98	29.30

Table 4. Mineralogical quantitative phase analysis of the analyzed binder fractions, obtained by full profile fitting of the experimental XRPD patterns according to the Rietveld method

6.7.2. SEM-EDS on binder fractions

PCA (Principal Component Analysis) was undertaken on the quantitative results from SEM-EDS done on the binder fraction of the samples. The biplot of the statistical treatment was obtained after log-transformation of the quantitative data, and represents 76.03% of the whole dataset variance. According to the biplot, the samples can be separated in three groups and two outliers.

Group 1

The first group is composed of the samples 2006, 2004, 3011. It is characterized by negative values of PC1 and PC2. The main element found in the matrix of this group is CaO testifying the prevalent aerial reaction in the mortars. Small quantities of Si and Al were also present in this group but their impact for the formation of C-A-S-H is not important. Furthermore, Mg aliquots are low, so they cannot give rise to M-S-H phases.

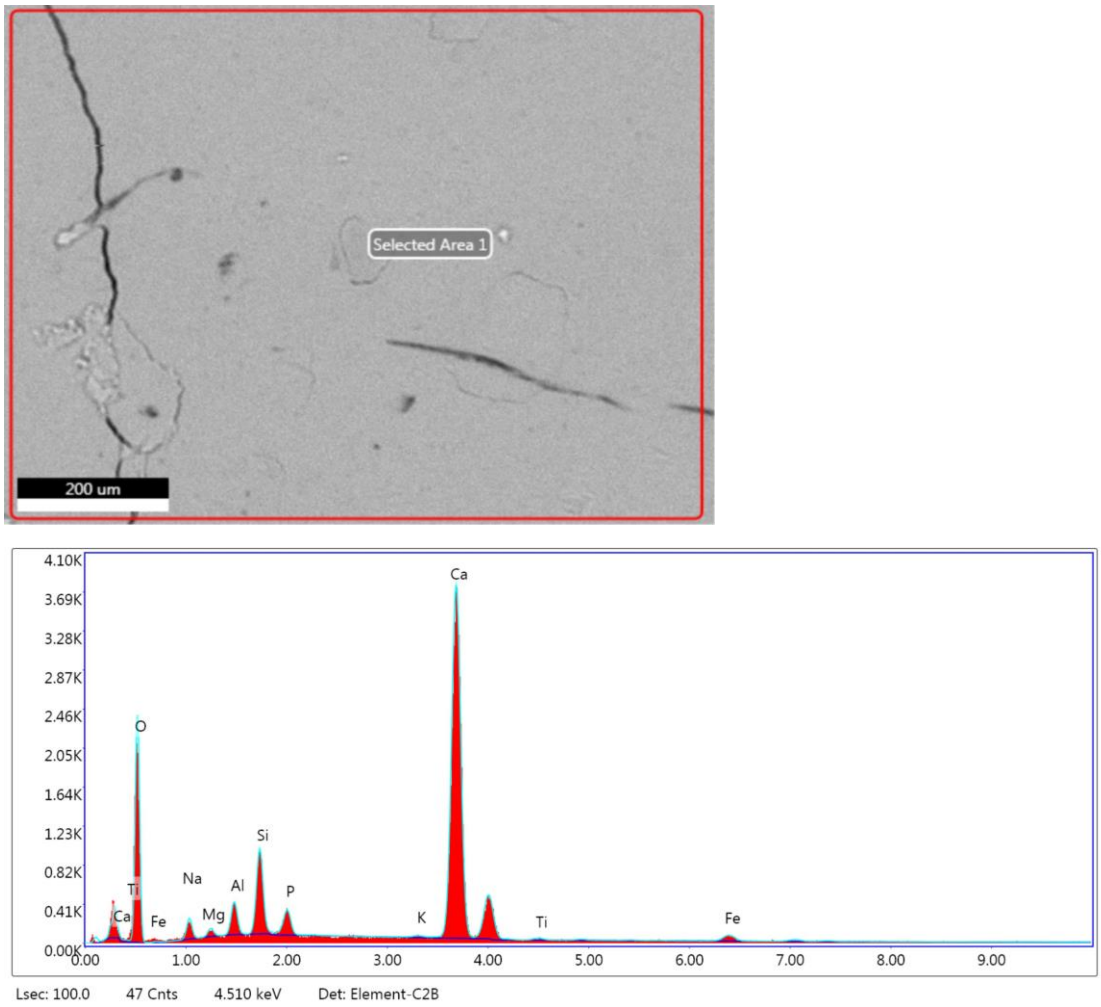

Figure 48. Binder fraction from the sample 2004. SEM-EDS image and spectrum

Group 2

In this group, there are positive values of PC2 and negative values of PC1. It includes two samples, 2003_S1 and 3002. Si and Al aliquots are firly high indicating the occurrence of C-A-S-H phases. Ca aliquots remain important, Mg content is medium.

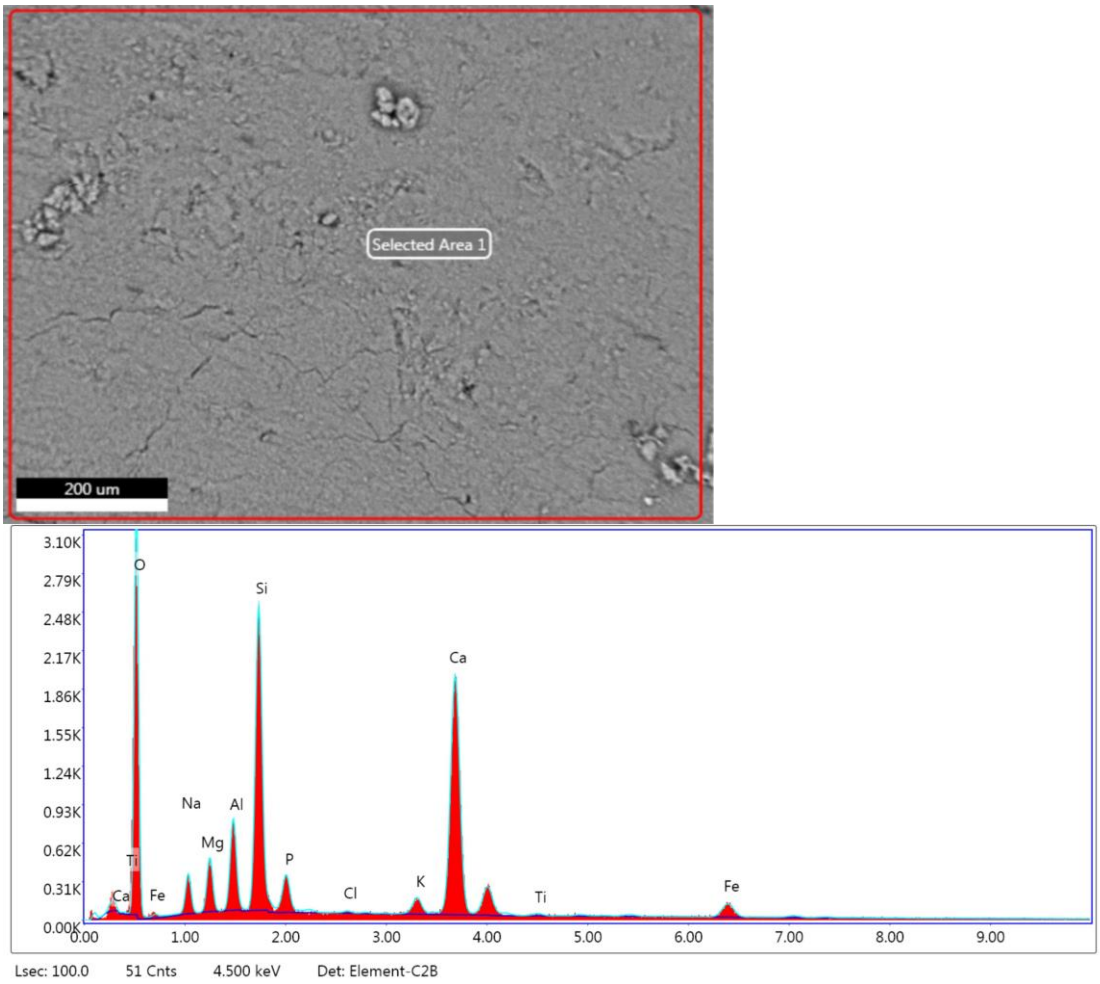

Figure 49. Binder fraction from sample 3002. SEM-EDS image and spectrum

Group 3

This group is described by positive values of PC1 and PC2. It is composed of the samples 1002_A3 and 3005. Ca aliquots are low, whereas Si and Al are quite significant compared to the rest of the groups. Their low content in Ca and the high amounts of Si and Al suggest the occurrence of a pozzolanic reaction and the formation of the poorly crystalline C-A-S-H phases. Their amount of Mg is important and it is testifying the occurrence of relevant M-A-S-H phase in the binder matrix.

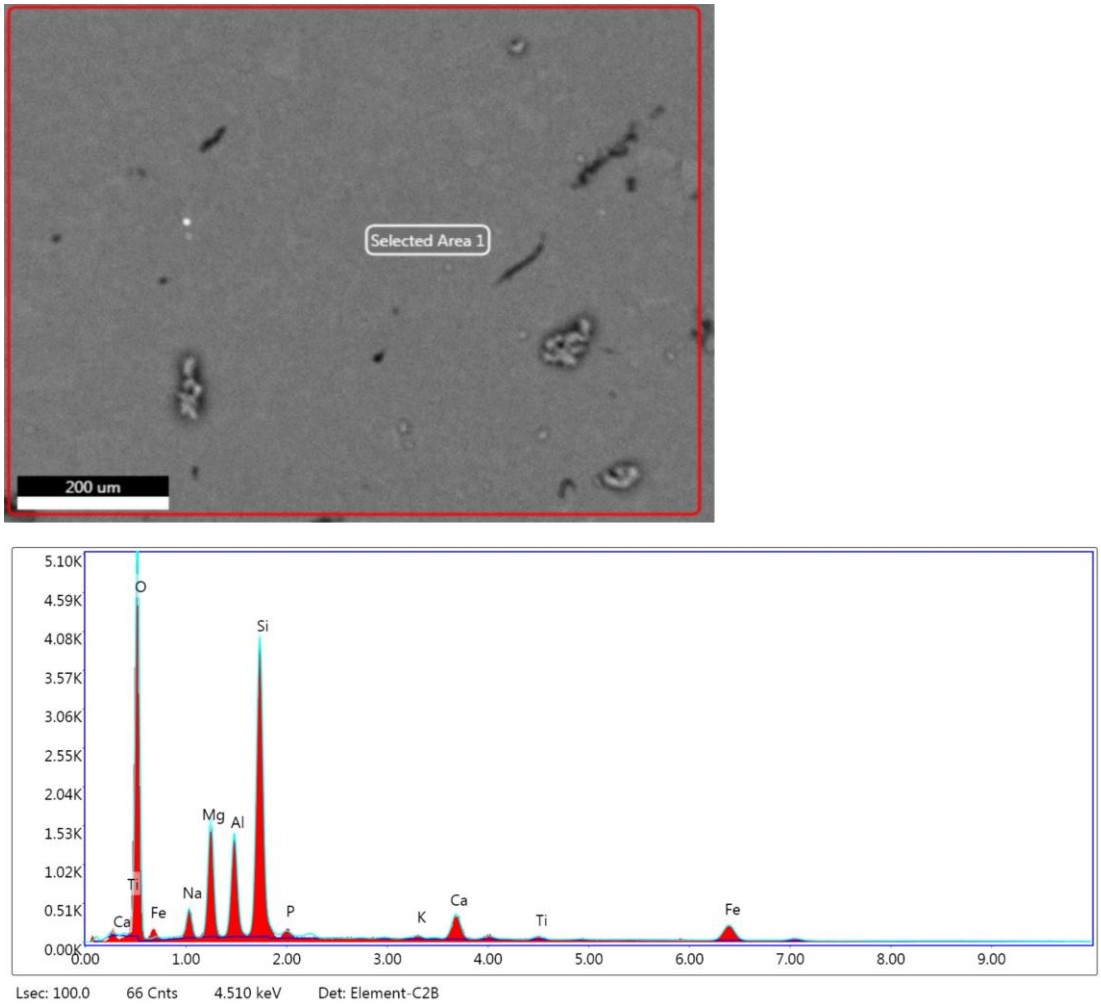

Figure 50. Binder fraction from the sample 1002_A3. SEM-EDS spectrum and image.

Outliers

The statistical treatment showed two outliers. The samples 1003 which came from the mortars of the rectangular blocks of the concrete pier have similar quantities in Si, Al and Ca with the third group which is described above. However, it has less quantity of Mg and a high quantity of Fe which has not been noticed in the groups. The next outlier is the sample 3003_AQ which came from the mortar of the pierced ashlar stones (Aqueduct stones) of the w3003 in the southern side of the Long Structure. Si and Al aliquots remain important, but Ca content is scarce. However, Mg can be described as pretty high compared to the rest of the samples indicating the occurence of M-A-S-H phases in the matrix. We can also suggest the partial addition of magnesian lime and/or dolomitic aggregates for the manufacture of the concrete of the aqueduct stones.

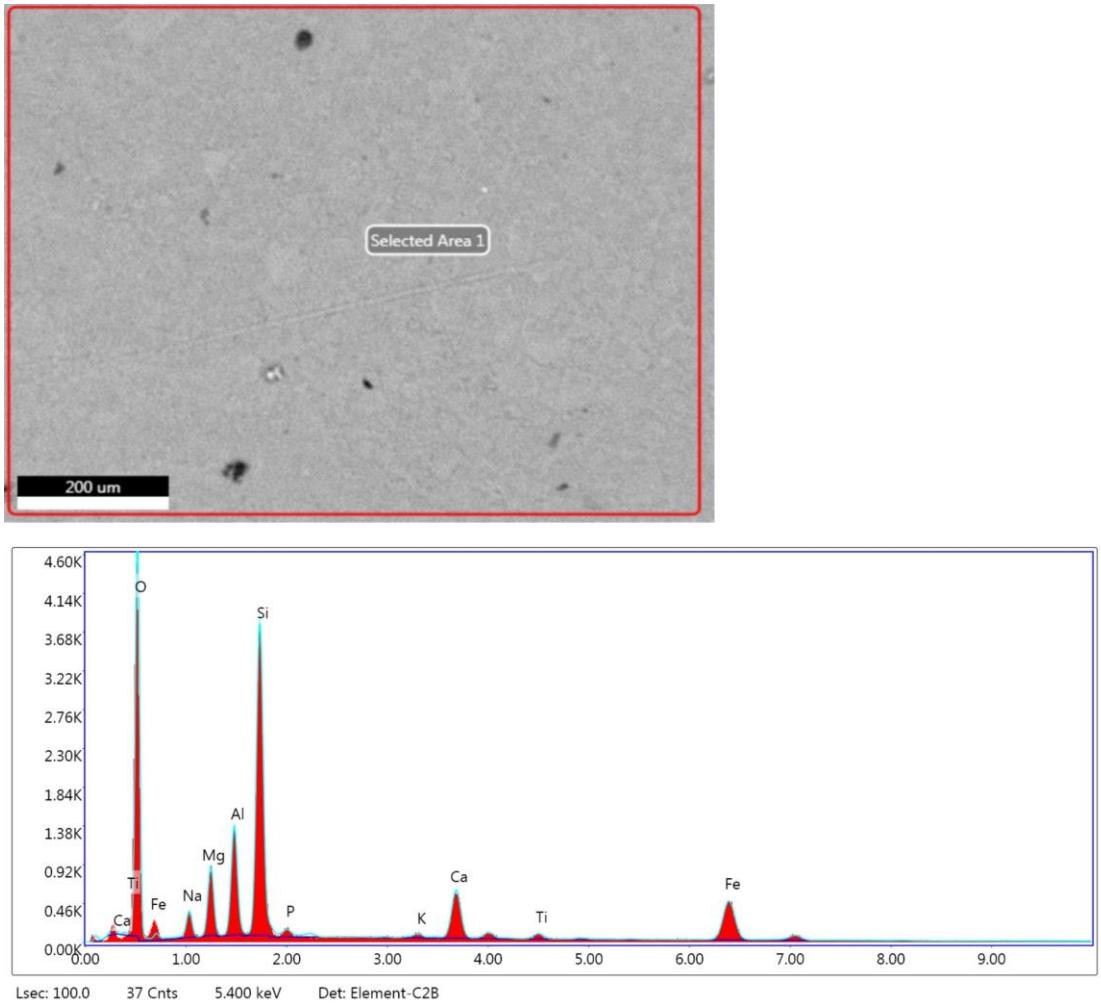

Figure 51. Binder fraction from sample 1003. SEM-EDS image and spectrum

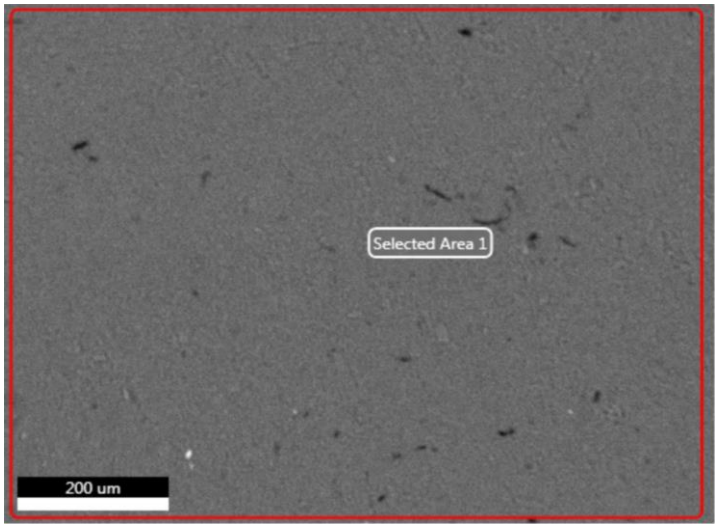

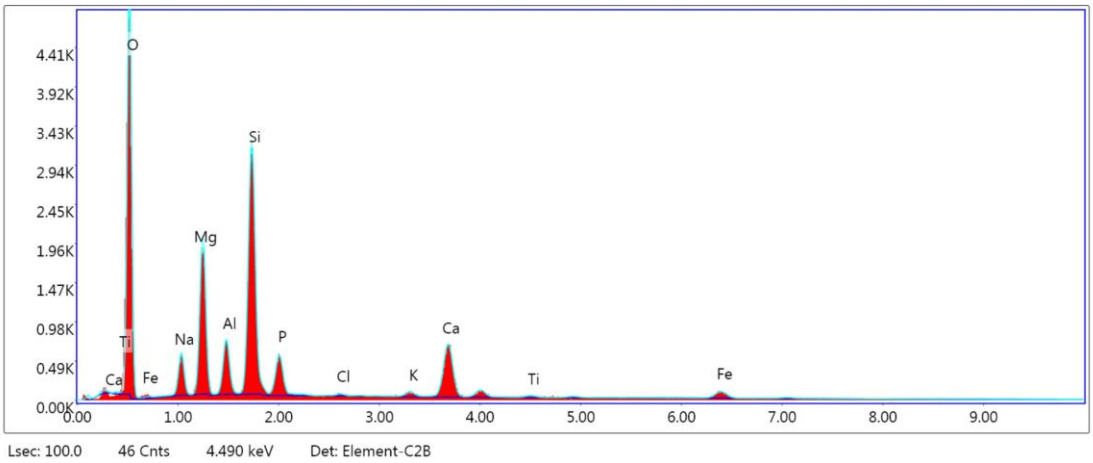

Figure 52. Binder fraction from sample 3003_AQ. SEM-EDS image and spectrum

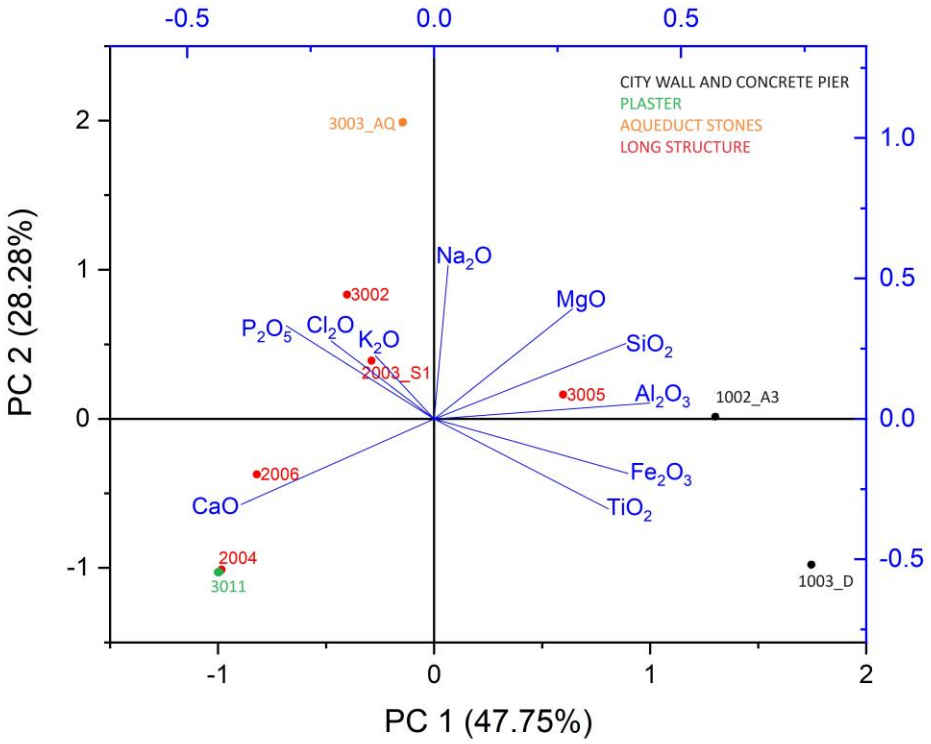

Figure 53. Biplot of the PCA (Principal Component analysis) of the semiquantitative data obtained from the analyzed binder fractions by SEM-EDS: the first two components have been plotted representing 76.03% of the total variance. Colors: Red=Long structure, Green=Plaster, Black=City Wall and Concrete pier, Orange=aqueduct stones

Mean

Sample	Na_2O	MgO	Al_2O_3	SiO_2	P_2O_5	Cl2O	K_2O	CaO	TiO_2	Fe_2O_3
1002A3	4.88	17.11	16.03	48.62	1.21	0.00	0.41	4.60	0.76	6.37
1003	4.44	9.91	15.31	44.85	1.03	0.00	0.53	7.98	1.18	14.77
2003	4.79	5.54	8.82	40.25	3.42	0.42	1.28	31.29	0.58	3.62
2004	4.21	1.24	5.41	13.08	5.08	0.06	0.29	67.44	0.53	2.66
2006	4.49	2.42	8.46	17.88	4.30	0.44	0.75	57.74	0.64	2.87
3002	5.84	6.45	10.41	33.75	5.51	0.24	1.49	31.94	0.42	3.95
3003Aq	7.28	21.94	8.94	38.74	9.57	0.26	0.58	9.51	0.41	2.76
3005	4.29	17.40	12.69	39.75	3.56	0.20	0.57	14.75	0.66	6.13
3011	3.48	1.12	5.51	14.92	6.01	0.06	0.67	64.52	0.57	3.13

Table 5. Mean values of the wt% of the elements measured in the binder fractions

Standard deviation

Sample	Na_2O	MgO	Al_2O_3	SiO_2	P_2O_5	Cl2O	K_2O	CaO	TiO_2	Fe_2O_3
1002A3	0.08	0.14	0.22	0.55	0.19	0.00	0.04	0.17	0.21	0.15
1003	0.24	0.19	0.08	0.09	0.23	0.00	0.03	0.25	0.12	0.10
2003	0.07	0.24	0.09	0.28	0.27	0.12	0.10	0.32	0.10	0.14
2004	0.40	0.11	0.19	0.16	0.10	0.10	0.12	0.23	0.01	0.11
2006	0.07	0.12	0.56	0.27	0.20	0.04	0.04	1.07	0.12	0.11
3002	0.15	0.28	0.40	1.13	0.46	0.08	0.05	1.12	0.07	0.29
3003Aq	0.36	0.19	0.09	0.20	0.11	0.05	0.07	0.19	0.08	0.22
3005	0.14	0.20	0.21	0.15	0.11	0.05	0.07	0.12	0.13	0.05
3011	0.57	1.00	0.21	0.10	0.24	0.11	0.04	1.70	0.13	0.14

Table 6. Standard deviation of the wt% of the elements measured in the binder fractions.

6.7.3. Combined PCA analysis on SEM-EDS and XRPD results of the binder fractions

In this PCA, we combined the data of the binder fractions both from XRPD and SEM-EDS analysis. In this case, the mineralogical and chemical results are combined in one PCA. We can observe in the new PCA figure that the samples are separated in three groups and one outlier.

Group 1

In the first group, we may notice the samples 2006, 2004, 3011, like the previous PCA analysis. It has negative values of PC1 and PC2. These samples are rich in Calcite

(CaO according to the chemical analysis) and poor in phyllosilicate gels. Therefore, the reaction occurred in the binders is mainly aerial and not pozzolanic.

Group 2

This group includes the samples which come from the City Wall (sample 1002_A3) and the concrete pier (1003_D). It has positive values of PC1 and both positive and negative values of PC2. As it has been noticed previously, these samples contain rich quantities of aluminosilicates and which they can give rise to the formation of C-A-S-H phases. Moreover, they are rich in Mg (dolomite) which comes from the salinity of the Sea of Galilee. The presence of Mg can form the creation of the paracrystalline M-A-S-H phases.

Group 3

The third group includes the samples 2003_s1, 3002 and 3005 which come from various walls of the Long Structure. They can be described as having positive values of PC2 and negative values of PC1, while only the sample 3005 has positive PC1 approaching the values of the second group. These samples have important content in Si, Al and Mg (phyllosilicate compounds and AFm) forming in this way C-A-S-H and M-A-S-H. Their quantity in calcite can be described as medium. The sample 3005 is quite different in this group, since it is compositionally similar to the samples from the second group parametrizing its hydraulic reaction as more relevant than the samples in the rest of the group.

Outlier 3003_AQ

This sample, as it was written previously, it has positive values f PC2 and negative values of PC1. It contains large quantities in MgO, Afm and amorphous phases. The occurrence of M-A-S-H and C-A-S-H phases can be characterized as significant. As it was suggested before, this sample may likely utilize a partially magnesian lime as binder.

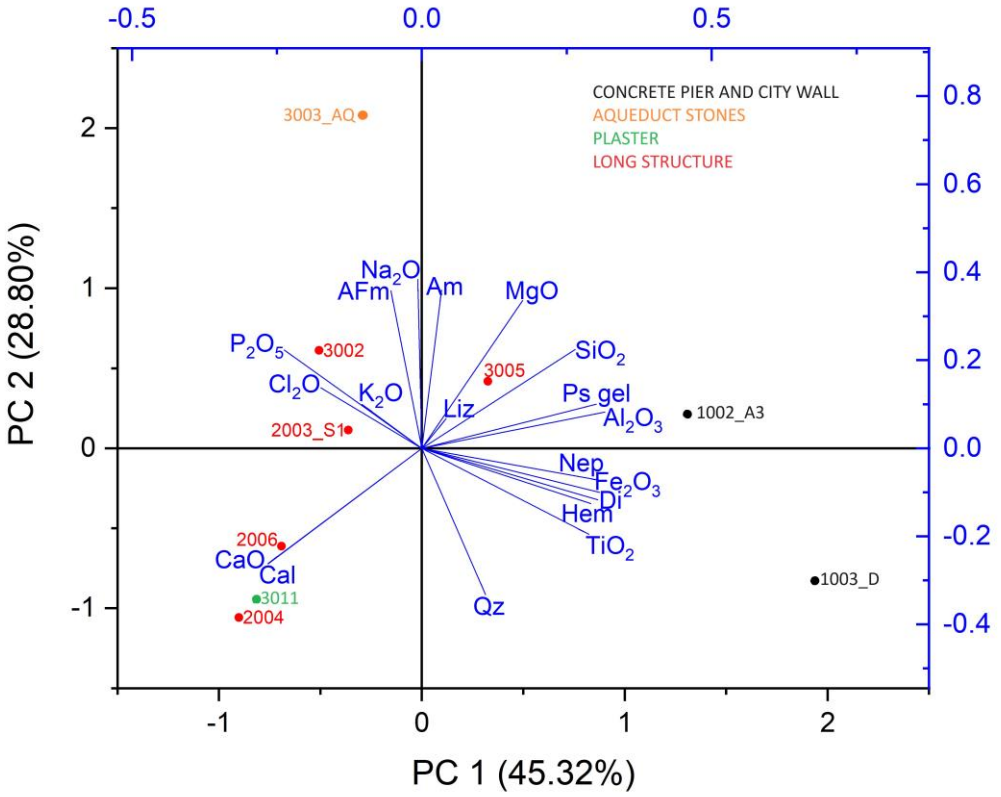

Figure 54. Biplot of the PCA (Principal Component analysis) of the quantitative data obtained from the analyzed binder fractions by both SEM-EDS and XRPD: the first two components have been plotted representing 74.12% of the total variance. Colors: Red=Long structure, Green=Plaster, Black=City Wall and Concrete pier, Orange=aqueduct stones. Abbreviations: Cal=calcite, Am=amorphous, Ps gel=phyllosilicate gels, Nep=Na-nepheline, Di=diopside, Hem=hematite, Qz=quartz

6.8. Colorimetry

The results from the colorimetry measurements are presented in the following table 8. The color variations among the mortar samples do not show significant differences. However, the mortar sample 1003 (concrete pier) appears to be quite different from the rest of the samples. Moreover, the plaster 3011 can be characterized as unique compared to the samples. Finally, the sample 3008 (sewer 3008-3009) seems to be distinctive from the rest of the color variations.

Sample	L*	a*	b*	Color	R	G	B
3002-PAV	69.5	2.3	7.7		180	168	156
3011	77.3	2.2	7.7		201	189	177
2001-DOOR	72.63	3.1	6.1		189	176	167
2001-F207	73.6	2.7	9.4		193	179	164
3001-S1	67.9	2.7	7.0		176	163	153
3003-FB	74.2	2.4	6.5		192	181	171
3010	75.4	2.5	8.3		197	184	171
L327	77.4	2.1	8.0		201	189	177
1002_A3	67.5	4.1	10.2		179	161	146
1003	62.7	6.6	17.1		174	147	122
1002_D	64.9	3.6	12.9		173	155	135
2001	68.7	5.4	9.3		184	164	151
2003-S1	72.9	2.8	8.4		191	177	164
2003-S2	72.8	5.7	10.0		196	175	161
2004	70.7	4.5	8.6		188	170	158
2005	74.5	2.9	9.1		196	181	167
2006	70.5	6.8	12.1		193	168	151
3002	77.9	2.8	8.7		205	190	177
3003-AQ	73.2	2.5	7.6		190	178	166
3004	74.9	3.5	10.6		199	182	165
3005	71.7	3.4	9.5		189	173	159
3006	71.4	3.9	10.8		190	172	155
3008-3009	70.2	6.4	17.2		192	167	141

Table 7. Colorimetry results of the powdered mortar samples

7. Discussion

After the chemical and the mineralogical analyses on the samples from the Long Structure and the extension of the City Wall in Tiberias, we have significant information about the composition of the mortars used for the construction of the structures in Myriam's Well beach.

7.1. Basalt aggregates

The use of basalt as an aggregate in the mortars of Myriam's Well beach in Tiberias can be justified by the fact that there are basalt outcrops in the nearby area. This way, the transportation of the raw material from the quarries to the site was much easier.

We should also refer to the benefits of basalt as an aggregate in the mortar pastes. It has been proven by chemical and mechanical experiments that basalt can be used as a filler in the OPC (ordinary Portland Cement). As a filler, basalt has a nucleating effect, accelerating the rate of hydration in the cement paste (El-Didamony H. et al. 2015, p. 267). By doing this, the cement paste filled with basalt can liberate more hydrated lime than the OPC which does not contain basalt. After 90 days of setting of the Cement paste filled with basalt aggregates, the basalt can work as a pozzolanic material due to the increase of OH ions liberated from the slaked lime (El-Didamony H. et al. 2015, p. 266). Then, the basalt absorbs an important quantity of OH^-, SO_4^{2-}, Ca^{2+} and K^+ and releases aluminates, silicates and Mg^{2+} to the lime solution forming in this way poorly crystalline C-A-S-H cementitious phases (El-Shahate Ismaiel Saraya M. 2014, p. 107, Dobiszewska M. and Beycioglu A. 2020, p. 12). The occurrence of M-A-S-H phases in the binders may come from the release of Mg^{2+} from the basalt rock. Probably, the builders in Tiberias were aware of the beneficial properties of basalt as an aggregate in mortar technology. Moreover, cement paste filled with basalt needs less water during the hydration process compared to the cement pastes filled with different aggregates (El-Didamony H. et al. 2015, p. 272). After experimental studies, it has been shown that the workability of the basalt aggregate is higher than that of the limestone aggregates because of the low absorption capacity of the basalt (Kishore L. S. et al. 2015, p. 41). Another important advantage of the cement paste filled with basalt is the increase of the compressive strength at later stages after 90 days (El-Shahate Ismaiel Saraya M. 2014, p. 109). The compressive strength of concrete filled with basalt aggregates has proven to be much higher than the compressive strength of OPC without any basalt additives (Siva Kishore et al. 2015, p. 41, Dobiszewska M. and Beycioglu A. 2020, p. 9), especially under the seawater (Binici H. et al. 2007, p. 1519). An increase in the compressive strength of the concrete can provoke a decrease of the abrasion which can affect it. Scholars have also found out that the basalt is responsible for the decrease of the porosity in cement, like any other pozzolanic material due to the decrease of air (El Didamony H. et al. 2014, p. 269, Dobiszewska M. and Beycioglu A. 2020, pp. 9-10). Therefore, mortars with basalt as an inert were a smart solution for the master builders even in ancient times, as they have similar properties as the mortars filled with natural or artificial pozzolanic materials.

The use of basalt aggregates with the combination of blast furnace slag has also suitable qualities for the concrete which is set underwater. Apart from the increase of the compressive strength which has been referred above, scholars have also demonstrated with experimental studies that the water permeability values of the concrete filled with basalt aggregates are low and the effectiveness of that kind of concrete against the chloride penetration can be significant (Binici H. et al. 2007, pp. 1519-1520, Dobiszewska M. and Beycioglu A. 2020, p. 11).

7.2. Salinity in the sea of Galilee

One other aspect that we should consider regarding the material technology of the mortars in Myriam's Well beach in Tiberias is the salinity of the sea of Galilee. The sea of Galilee is a lake with a high percentage of salinity, which varies from 190 to 280 mg L^{-1} Cl^- (Rimmer A. and Nishri A. 2014, p. 113), since there are underground

salt water sources which provide the lake with saline water (Kolodny Y. et al. 1999, p. 1035-36). The major saline water springs are located in the western side of the Lake Kinneret. Some of the groups of springs with saline water are those which are located in Tiberias, Tabgha, Fuliya and Barbutin (Kolodny Y. et al. 1999, p. 1044, Rimmer A. and Nishri A. 2014, p. 144). The vicinity of the Long Structure close to the lake water plays a significant role in the composition of the concrete. Even more, structures like the extension of the City Wall and the concrete pier which are underwater or attached to the lake are affected more intensely by the lake environment.

7.3. Materials Technology and pozzolanicty

As it was shown from the results of the mineralogical and chemical analyses, a number of mortar samples were rich in Mg and dolomite. The presence of Mg in the binder mixture can be associated with the addition of combustion residues from organic matter, like burnt dung, in the binder mixture. The addition of combustion residues from organic matter is an intentional technological choice, since they are characterized by pozzolanic material (Secco M. et al. 2020, p. 79). That practice was common in the binding composites of Phoenician-Punic and Roman sites in north Africa and the Levantine regions (Lancaster L. C. 2012, Secco M. et al. 2022, p. 15). Except of their content in Mg, ashes from organic matter contain Si as a major component, Al, CaO and Fe_2O_3. The presence of animal ashes can be confirmed by the occurrence of calcium phosphates as it is demonstrated by the SEM-EDS analyses and the occurrence of apatite (Secco M. et al. 2022, p. 16).

The sea of Galilee is a freshwater lake with a high percentage of salinity, as some of the water sources of the lake are salty. The small quantities of Na and Cl found in the samples from Myriam's Well beach may be related with the addition of the lake's partially salt water during the mortar preparation (Secco M. et al. 2020, p. 80). The presence of salt (NaCl) in the mortars can increase the pH value which can lead to an increase in silica dissolution. The rise of pH is promoted by the formation of sodium hydroxide in binders after the interaction between calcium hydroxide and sodium chloride (Secco M. et al. 2020, p. 80, 2022, p. 18). Moreover, the compressive strength of the mortars can rise due to the high pH value, and the formation of the calcium-sodium silicate gel can make the cementation process faster than the calcium silicate gel (Karim M. E. et al. 2017, p. 8). The occurrence of salt water in the binder matrix together with the combustion residues of animal origin can lead to the formation of the M-A-S-H phyllosilicate gel because of their quantity in Mg. All the examined samples have small quantities of dolomite which can be related to the high Mg activity in combination with sulphate-reducing bacteria activity in the lake environment (Secco M. et al. 2022, p. 18).

7.4. Cocciopesto mortars in Myriam's Well beach

Apart from the use of ash mortars in Myriam's Well beach, there was also an utilization of cocciopesto mortars (mortars filled with ceramic fragments) for parts of the City Wall, the concrete pier and the some of the walls of the concrete structure. The presence of hematite found in the XRPD analysis may confirm the presence of ceramics in the binders (Secco M. et al. 2018, p. 198). Ceramic fragments are visible in the binder through petrographic study with the use of Optical Microscopy as

reddish inclusion with quartz particles and a microcrystalline matrix. As it was written above, they are composed of aluminosilicate compounds which can react with the lime and form the C-A-S-H phases which give to the concrete perfect durability and mechanical properties (Seymour L. et al. 2022, p. 8).

The use of ceramic fragments in the mortars initiated during prehistoric times in the Mediterranean for lining of cisterns and other structures which came in contact with the water. During the early Imperial period and more specifically during the building of Santa Liberata's and Caesarea's harbor, there was a utilization of concrete filled with pozzolana from the Gulf of Naples and ceramic fragments which was set underwater for the construction of the quays (Vola G. et al. 2011, p. 327). The use of ceramics in mortars which contained a high amount of volcanic tuff and pumice as natural pozzolanic material proves that there was an awareness during the Early Imperial period about the hydraulicity of cocciopesto mortars set underwater. Moreover, the ceramic fragments partially replaced the pozzolana aggregates which could not be available in great abundance, and their transportation in large quantities from the region of Pozzuoli to Caesarea seemed difficult and costly. Ceramics were always available and can be used in large quantities.

7.5. Construction phases

The chemical and mineralogical analyses have allowed us to separate the walls of the City Wall and the Long Structure in different construction phases. The observation in the construction technique of the walls can also be beneficial to the division of the buildings in different phases. However, the construction phases which are described here are not dated with the method of ^{14}C and they are not presented in a chronological order.

Construction phase 1

The walls 2001 and 2006 are built with the use of regular basalt ashlar stones. The composition of the hydraulic concrete from these walls seems similar. According to the quantitative analyses by XRPD, the mortar samples from these walls belong to the same group as indicated by PCA analysis. Moreover, the sample 2001 "door" belongs to the same group. This shows to us that the "entrance" of that wall was closed possibly lightly after the construction of the W2001. Optical microscopy demonstrated that the samples from this group have the same composition in ceramic fragments added as an artificial pozzolanic material. SEM-EDS analyses showed that the samples were rich in Ca but their Si and Al content varies from moderate to poor.

Even though sample 2004 belongs to the same group and has the same composition as the rest of the samples, it is difficult to place it in the same construction phase. The wall 2004 was built with a different technique with respect to W2006 and W2001, with the use of irregular basalt stones. Sample 2003_s2 belongs to the same group of samples as 2001 and 2006. However, the wall 2003 is built in a different way from the walls 2001 and 2006, so it could not belong to the same construction phase. The wall

2003 resembles the wall 2004 in its way of construction, built with irregular basalt blocks. Therefore, this group of samples can be divided into two construction phases. The first phase contains the samples taken from the walls 2001 and 2006 and the second one includes the samples 2004 and 2003_s2.

Regarding the sample 2001_F207, it has a mineralogical composition different from the samples of this construction phase. Furthermore, its microscopic appearance is also distinctive, since the ceramic fragments of this sample are absent and only some ash particles have been noticed. However, it is likely that the samples taken from the steps should also be included in the same construction phase of the entrance in 2001, since it is more possible that they were built during the construction of an entrance. A possible rebuilding of the steps after the establishment of W2001 and W2006 could be proposed as well.

Construction phase 2

The samples taken from the city wall and the concrete pier show similar mineralogical and chemical composition. According to the quantitative analysis carried out by XRPD and the statistical treatment by PCA, these samples are part of the same group. The analysis done by optical microscopy showed that the samples of this group have similar characteristics of the binding matrices and affine composition of the aggregates. SEM_EDS analysis indicated a high quantity of Si, Al and Mg and a low Ca content, indicating the development of C-A-S-H and M-A-S-H phases in the binders.

On the other hand, s1001, taken from the limestone wall 1001 shows a FTIR spectrum with a low silicate peak and high carbonate peak. Therefore, w1001 may belong to a different construction phase or it was built with an aerial mortar, because the use of hydraulic mortar for this wall is not necessary, since it is located in the western side of Myriam's Well beach and is not directly affected by the moisture of the lake environment.

Construction phase 3

The walls 3001, 3002, 3010 and 3011 can be grouped into the same construction phase. Even though the sample 3010 belongs to a different group according to the quantitative analysis by XRPD, its composition is slightly different from the rest of the samples. Also, the wall 3010 was built near the wall 3011. Both walls were constructed vertical to the wall 3002 on its western side. Moreover, the plaster piece found in L327 was possibly part of the wall 3010, since this locus was excavated in a very close distance to that wall. The optical microscopy study showed a similar composition for the samples taken from these walls. SEM_EDS indicated that the samples were rich in Ca and poor in aluminosilicate compounds, which is the proof of the use of aerial mortar for these walls. The walls are not located near the lake water, so the use of hydraulic concrete was not necessary in that case.

Construction phase 4

The fourth construction phase is related to the samples 3005, 2005, 3006, 3004 and 2003_s1. From an architectural point of view three walls, W3005, W3006 and

W3004, are connected to each other forming a rectangular space. Moreover, their binder composition seems similar according to the XRPD quantitative analysis. W2005 was built probably during the same period with these walls, and it is located parallel to W2004. The construction of the W2005 parallel to W2004 could have served a specific function related to the activities in the lake. However, we cannot be sure which wall predates each other. Sample 2003_s1 is grouped together with these samples and is quite different from the sample 2003_s2, which belongs to the construction phase 1. We can propose that the W2003 was partially rebuilt using different technological skills in its concrete's composition. Mortar sample 2003_s2 contains ceramic fragments which was added as an artificial pozzolanic material giving the mortar hydraulic properties, while sample 2003_s1 contains inorganic tissues of biogenic origin which may come from combustion residues from organic matter like dung or plants.

Construction phase 5: Aqueduct stones in W3003

As it was shown by the chemical and mineralogical analyses, the mortar of the aqueduct stones is composed of lime and ash, probably from burnt dung or plants. According to the composition of the mortar in the W3003, we can estimate the dating without the use of ^{14}C method. The mortar of the aqueduct stones was set in multiple layers (at least two layers). From a macroscopic point of view the outer layer is more whitish, while the inner layer is grayish because of its high amount of combustion residues of organic matter. This way, we can suggest that the construction of the pierced ashlar stones and their cement occurred during the 1st century AD (Porath Y. 2002, p. 35). However, this estimation is based on Porath's macroscopic view on the cement materials of aqueducts without any chemical or mineralogical analysis.

Regarding the mortar samples from the fallen blocks which were placed on top of the aqueduct stones, they appear to be quite distinct from the mortars in the aqueduct stones. The mortar from these rectangular blocks is fat, while the mortar of the aqueduct stones is lean, rich in basalt aggregates and clasts. Also, there is a difference in the matrix of the mortar from a microscopic view. The matrix of the sample 3003_AQ is more brownish, whereas the matrix from 3003_FB is more grayish. According to the statistical treatment sample 3003_AQ is an outlier and sample 3003_FB belongs to a separate group. However, I believe that the placement of the pierced ashlar blocks in W3003 can be grouped into the same construction phase with the construction of the rectangular blocks. The hydraulic mortar from the aqueduct stones can have been manufactured since the time when the aqueduct was constructed. It should be associated possibly with the aqueduct which was located in Tiberias and was probably destroyed during the earthquake of 8th century CE. The mortar from the blocks can have been manufactured during the construction of W3003 when the pierced ashlar stones from the aqueduct were placed under the rectangular blocks. Therefore, both the aqueduct stones and the rectangular blocks of W3003 are part of the same construction phase.

Construction phase 6: Sewer

The sewer (w3008-3009) is a separate construction phase. Although the sample 3008 is grouped within the 3rd group according to the XRPD quantitative analysis, its

microscopic appearance is quite different from the rest of the samples of the Long Structure. After the colorimetry measurements, it was noticed that the color values of the specific samples are unique compared to the rest of the mortars. The mortar of the sewer was made with the addition of clay as a pozzolanic material. Ceramic fragments or combustion residues of organic matter were not detected after the micromorphological study of the sample.

Construction phases	**Walls (City wall, concrete pier and Long Structure)**
Construction phase 1	First subphase. W2001, 2001_F207, W2006
	Second subphase: W2003, W2004
Construction phase 2	W1001, W1002 (city wall), W1003 (concrete pier)
Construction phase 3	W3001, W3002, W3010, W3011 (plaster), L327 (plaster)
Construction phase 4	W2005, W2003, W3004, W3005, W3006
Construction phase 5	W3003 (Aqueduct stones and rectangular blocks)
Construction phase 6	W3008-W3009 (Sewer)

Table 8: Construction phase and walls from the city wall, concrete pier and Long Structure

7.6 Association of the lake level fluctuations with the City Wall and the concrete pier

The sea of Galilee experienced sharp fluctuations regarding its water level during the Holocene. It is believed that the fluctuations of the lake level may have affected the construction of the City Wall and the concrete pier which is underwater. Therefore, the manufacture of the hydraulic concrete for these structures may have been influenced by the lake drops or rises. Before referring to the lake levels during the historic period, we should mention the level during the excavation periods in 2020 and 2021. From the end of October until the middle of December 2021 the lake level varied from 210.635 to 210.78 mbsl. The last year and more specifically from the end of November until the beginning of December 2020 the lake level varied from 209.98 to 209.96 mbsl (Nantet E. 2021, p. 6).

During the Holocene, a significant rise of the lake level was noticed during the late Hellenistic-early Roman period which was estimated from 210.30 to 208.30 mbsl (Giaime M. and Artzy M. 2022, p. 4). A drop of the lake level occurred during the second half of the 3rd century which reached 210 mbsl. During the 5th – 6th century, the mean maximum lake level decreased to 213.84 mbsl. A new increase in lake level happened during the late 8th century due to an earthquake (Giaime M. and Artzy M. 2022, p. 6). We can conclude that today's lake level is more or less similar to that one of the Late Hellenistic/early Roman period.

The changes in the lake level seem variable. The structures in Myriam's Well beach were built during the Byzantine-Early Islamic period according to the findings of the excavations. This period can be characterized by a significant drop in the lake level and a rise which followed after the earthquake in the 8th century. However, the concrete pier was probably built on land during Fall and submerged later (maybe partially) when the lake level rised. The composition of the concrete used for the construction of the concrete pier is rich in phyllosilicate gels which is an indication of a pronounced pozzolanic reaction in the binder. As a result, it was given attention to its pozzolanicity since it had to resist water erosion. Moreover, the discovery of the traces of wood around the easternmost concrete block demonstrates to us that the builders used one of the techniques of the wooden formwork as described by Vitruvius (Vitr. 5.12.3). These techniques were quite known for underwater structures, like quays. The function of the rectangular concrete blocks from the concrete pier was probably a support for a platform used as a quay or as a foundation for a part of the wall which intruded into the lake.

The reason why the City Wall and the concrete pier were built on the lake side has been referred above. Magdala was shaken by Tito's troops from the lake side, as it was unprotected by a City Wall (Josephus, *De bello Ioudaico*, III.10.5). On the other hand, Tiberias' authorities were aware of an easy passage from the lake side, so they reinforced that part with a new fortification.

8. Conclusions

The mineralogical and chemical analyses on the mortars in Myriam's Well beach showed that they are extremely heterogeneous materials, and the study allowed differentiating the structures into building phases according to the binders' composition The architectural analysis of the Long Structure, the extension of the City Wall and the concrete pier which is studied by the master student Maxence Marques also indicated that there are different construction phases in the structures. As a result, the structures were separated into five construction phases.

The chemical and mineralogical examination of the mortar samples demonstrated different aspects of mortar technology and pozzolanicity. The use of basalt aggregates as a filler in the mortars of Myriam's Well beach showed perfect durability and mechanical properties for the mortars. The delayed pozzolanic reaction of the basalt particles with the lime in a water-saturated environment has been proven to be beneficial for filling the pores in the binders and increase its mechanical and durability properties. Moreover, the mortars became more resistant to the water erosion.

The salinity of the sea of Galilee which is originated from saltwater sources in its western side has also affected the chemical and mineralogical composition of the samples. The occurrence of M-A-S-H phases (magnesium aluminosilicate hydrates) in the binders is the result of the use of the lake's water in the preparation of the mortars and the contact of the water with the structures in Myriam's Well beach.

The study of the composite materials of the Myriam's Well beach has demonstrated the simultaneous utilization of different mortar technology traditions. On one hand, part of the walls of the Long Structure and the extension of the City Wall were built with cocciopesto mortars (mortars with ceramic fragments or powder). Cocciopesto mortars is a technological tradition originating from the Greek-Roman world. On the other hand, some mortars were manufactured with the addition of combustion residues from organic matter, typical tradition in the Levantine region and North Africa.

Finally, the use of hydraulic mortar especially in the concrete pier and the city wall is associated with the lake level fluctuations which affected the construction of the buildings. The mortars of the concrete pier and the city wall have been described by the significant occurrence of C-A-S-H and M-A-S-H phases. The pozzolanicity of these mortars has demonstrated that they were close to the lake water (for the eastern part of the City Wall) or they were constructed underwater with the help of wooden formworks (rectangular blocks of the concrete pier). Therefore, the builders of the city wall and the concrete pier gave attention to the materials used for the manufacture of the mortars in the northern part of Myriam's Well beach, since they noticed the lake level elevations of that period, even though they were lower than today's elevations.

9. Bibliography

Historical sources

C. Pliny Secundi, *Naturalis Historiae Libri XXXVII* (eds. C. Mayhof, C. Pliny Secundi, Naturalis Historiae Libri XXXVII, Leipzig, 1892)

Flavius Josephus*, De bello Iudaico, Books IV-VII* (eds. H. Thackeray, Josephus, The Jewish War, Books IV-VIII, Cambridge, 1968)

Nasir-i Khusrau, *Book of travels* (eds. E. Yarshater, Naser-e Khosraw's Book of Travels, transl. W. M. Thackston, in Persian Heritage Series Number 36, New York, 1986)

Procopius, *De Aedificiis* (eds. J. Haury, Procopi Caesariensis Opera Omnia, vol. 4, Leipzig, 1964)

Pollux, *Nomenclature* (eds. E. Becker, Iulii Pollucis Onomasticon, Berlin, 1846)

Strabo, *Geographia* (eds. A. Meinek, Strabonis Geographica, Leibzig, 1877)

Theophrastus, *De Lapidibus* (eds. E. R. Caley and J. C. Richards, Theophrastus On Stones. A modern edition with Greek Text, Translation, Introduction and Commentary, Ohio, 1956)

Vitruvius, *De Architectura* (eds. I. Rowland, T. Howe, M. Dewar, Vitruvius: Ten books on Architecture. Cambridge, 1999)

Scientific sources

Addis, A., Secco, M., Marzaioli, F., Artioli, G., Arnau, A., Passariello, I., Terrasi, F., Brogiolo, G. 2019. Selecting the Most Reliable 14C Dating Material Inside Mortars: The Origin of the Padua Cathedral. Radiocarbon, 61 (2), pp. 375-393. doi:10.1017/RDC.2018.147

Artioli, G., Secco, M., Addis, A., 2019. The Vitruvian legacy: mortars and binders before and after the Roman world, in: Artioli, G. and Oberti, R. (eds) EMU Notes in Mineralogy, 20, 4, pp. 151–202.

Avi-Yonah, M., 1950-51. The Foundation of Tiberias. Israel Exploration Journal, 1, 3, 160-169.

Avni, G., 2014. The Byzantine-Islamic Transition in Palestine: An Archaeological Approach, Oxford University Press

Asscher, Y., Van Zuiden, A., Elimelech, C., Gendelman, P., 'Ad, U., Sharvit, J., Secco, M., Ricci, G., Artioli, G. 2020. Prescreening Hydraulic Lime-Binders for Disordered Calcite in Caesarea Maritima: Characterizing the Chemical Environment Using FTIR. Radiocarbon, 62 (3), pp. 527-543. doi:10.1017/RDC.2020.20

Baragona, A., J., Zanier, K., Frankova, D., Anghelone, M., Weber, J., 2022. Archaeometric analysis of mortars from the Roman Villa Rustica at Scolarice (Slovenia). Annales, Annals for Istrian and Mediterranean Studies, Series Historia et Sociologia, 32, 4, pp. 499-522

Brandon, C. J., Hohlfelder, R. L., Jackson, M. D., Oleson, J. P. (Eds), Bottalico, L., Cramer, S., Cucitore, R., Gotti, E., Stern, C. R., Vola, G., 2014. Building for eternity: the history and technology of Roman concrete engineering in the sea, Oxford England, Havertown Pennsylvania

Brandon, C. J. and Hohlfelder, R. L., 2014. History and procedures of the ROMACONS Project in J. P. Oleson (eds) Building for eternity: the history and technology of Roman concrete engineering in the sea. Oxford England, Havertown Pennsylvania. pp. 37-54.

Brandon, C. J., 2014. Roman formwork used for underwater construction in J. P. Oleson (eds) Building for eternity: the history and technology of Roman concrete engineering in the sea. Oxford England, Havertown Pennsylvania. pp. 189-222.

Binici, H., Aksogan, O., Bahsude Goru, E., Kaplan, H., Nuri Bodur, M., 2008. Performance of ground blast furnace slag and ground basaltic pumice concrete against seawater attack. Construction and Building Materials 22, pp. 1515–1526

Dilaria, S., Previato, C., Bonetto, J. Secco, M., Zara, A., De Luca, R., Miriello, D., 2023. Volcanic Pozzolan from the Phlegraean Fields in the Structural Mortars of the Roman Temple of Nora (Sardinia). Heritage, 6, pp. 567–586. https://doi.org/10.3390/heritage6010030

Dobiszewska, M., Beycioglu, A., 2020. Physical Properties and Microstructure of Concrete with Waste Basalt Powder Addition. Materials 13 (16) 3530. https://doi.org/10.3390/ma13163503

El-Didamony, H., Helmy, I., Osman, R. M., Habboud, A., 2015. Basalt as Pozzolana and Filler in Ordinary Portland Cement. American Journal of Engineering and Applied Sciences, 8 (2), pp. 263-274. https://doi.org/10.3844/ajeassp.2015.263.274

El-Shahate Ismaiel Saraya, M., 2014. Study physico-chemical properties of blended cements containing fixed amount of silica fume, blast furnace slag, basalt and limestone, a comparative study. Construction and Building Materials 72, pp. 104-112.

Giaime, M., Artzy, M., 2022. Using archaeological data for the understanding of Late-Holocene Sea of Galilee's level fluctuations. Scientific Reports 12, 9775. https://doi.org/10.1038/s41598-022-09768-8

Gertwagen, R., 1988. The Venetian port of Candia, Crete (1299-1363): Construction and Maintenance. Mediterranean Historical Review, 3:1, pp. 141-158 https://doi.org/10.1080/09518968808569543

Hirschfeld, Y., 1992. A Guide to antiquity sites in Tiberias, Israel Antiquities Authorities, Jerusalem

Hirschfeld, Y. 1999. Imperial Building Activity during the reign of Justinian and Pilgrimage to the Holy Land in light of the excavations of Mt. Berenice, Tiberias. Revue Biblique, 106, 2, pp. 236-249

Hohlfelder, R. L., 1988. Procopius, de aedificiis, 1.11.18–20: Caesarea maritima and the building of Harbours in late antiquity. Mediterranean Historical Review, 3:1, pp. 54-62 https://doi.org/10.1080/09518968808569537

Hohlfelder, R. L., Brandon, C. J., 2014. Narrative of the ROMACONS fieldwork in J. P. Oleson (eds) Building for eternity: the history and technology of Roman concrete engineering in the sea. Oxford England, Havertown Pennsylvania. pp. 55-101

Horgnies, M., Chen, J. J., Bouillon, C., 2013. Overview about the use of Fourier Transform Infrared spectroscopy to study cementitious materials, Materials Characterisation VI, pp. 251-262

Jackson, M. D., Vola, G., Gotti, E., Zanga, B., Sea water concretes and their material characteristics in J. P. Oleson (eds) Building for eternity: the history and technology of Roman concrete engineering in the sea. Oxford England, Havertown Pennsylvania. pp. 141-187.

Karim, M. E., Alam, J., Hoque, S. 2017. Effect of salinity of water in lime-fly ash treated sand. International Journal of Geo-Engeneering 8:15, DOI 10.1186/s40703-017-0052-0

Kishore, I. S., Mounika, L., Prasad, C. M., Krishna, B. H., 2015. Experimental Study on the Use of Basalt Aggregate in Concrete Mixes. SSRG International Journal of Civil Engineering (SSRG-IJCE) – volume 2 Issue 4, pp. 39-42 DOI: 10.14445/23488352/IJCE-V2I4P107

Kolodny, Y., Katz, A, Starinsky, A., Moise, T., 1999. Chemical tracing of salinity sources in Lake Kinneret (Sea of Galilee), Israel. Limnology Oceanography 44 (4), pp. 1035-1044

Lancaster, L.C. 2012. Ash mortar and vaulting tubes: agricultural production and the building industry in North Africa in S. Camporeale, H. Dessales, A. Pizzo (eds), Arqueología de la Construcción III: Los Procesos Constructivos en el mundo Romano: La Economía de las Obras (École Normale Supérieure, Paris, 10-11 de diciembre de 2009), Madrid-Merida, pp. 146-290.

Maravelaki-Kalaitzaki, P., Bakolas, A., Moropoulou, A., 2003. Physico-chemical study of Cretan ancient mortars. Cement and Concrete Research 33, 5, pp. 651–661 http://dx.doi.org/10.1016/S0008-8846(02)01030-X

Maor, Y., Toffolo, M. B., Feldman, Y., Vardi, J., Khalaily, H., Asscher, Y., 2023. Dolomite in archaeological plaster: An FTIR study of the plaster floors at Neolithic Motza, Israel, Journal of Archaeological Science: Reports, 48, 103862 https://doi.org/10.1016/j.jasrep.

Navarro-Mendoza, E.G., Alonso-Guzman, E.M., Sanchez-Calvillo, A., Bedolla-Arroyo, J.A., Becerra-Santacruz, H., Navarro-Ezquerra, A., Gonzalez-Sanchez, B.,

Martinez-Molina, W., 2023. Physical and Mechanical Characterization of Lime Pastes and Mortars for Use in Restoration. Heritage, 6, pp. 2582-2600. https://doi.org/10.3390/heritage6030136

Nantet, E., 2020. South Tiberias Excavations 2020: Winter season (February 2nd–22nd), Fall season (November 22nd–December 10th) [unpublished].

Nantet, E., 2021. South Tiberias Lake Area (at Myriam's well beach): Underwater Excavation (June 20th – July 8th), Land Excavation (November 21st – December 17th) [unpublished].

Oleson, J. P., 2014. Ancient Literary sources concerned with Roman concrete technology in J. P. Oleson (eds) Building for eternity: the history and technology of Roman concrete engineering in the sea. Oxford England, Havertown Pennsylvania. pp. 11-36.

Oleson, J. P. and Jackson, M. D., 2014. The technology of Roman Maritime Concrete in J. P. Oleson (eds) Building for eternity: the history and technology of Roman concrete engineering in the sea. Oxford England, Havertown Pennsylvania. pp. 1-10

Pecchioni, E., Fratini, F., Cantisani, E., 2014. Atlas of the ancient mortars in thin section under optical microscope, Florence

Porath, Y., 2002. Hydraulic Plaster in Acqueducts as a Chronological Indicator. In D. Amit, J. Patrich and Y. Hirschfeld (eds). The Acqueducts of Israel [Journal of Roman Archaeology Supplementary Series 46]. Portsmouth. pp. 25–36.

Puertas, F., Palacios, M., Manzano, H., Dolado, J. S., Rico, A., Rodríguez, J., 2011. A model for the C-A-S-H gel formed in alkali-activated slag cements, Journal of the European Ceramic Society, 31, 12, pp. 2043-2056, https://doi.org/10.1016/j.jeurceramsoc.2011.04.036

Rimmer, A., Nishri, A., 2014. Salinity. in T. Zohary, A. Sukenik, T. Berman, & A. Nishri (Eds.), Lake Kinneret: Ecology and management, Springer Heidelberg, pp. 113-131.

Regev, L., Zukerman, A., Hitchcock, L., Maeir, A. M., Weiner, S., Boaretto, E. 2010. Iron Age hydraulic plaster from Tell es-Safi/Gath, Israel, Journal of Archaeological Science, 37, 12, pp. 3000-3009 https://doi.org/10.1016/j.jas.2010.06.023

Secco, M., Dilaria, S., Addis, A., Bonetto, J., Artioli, G., Salvadori, M., 2018. The evolution of the Vitruvian recipes over 500 years of floor making techniques: the case study of the Domus Delle Bestie Ferite and the Domus di Tito Macro (Aquileia, Italy). Archaeometry 60, 2, pp. 185-206. doi: 10.1111/arcm.12305

Secco, M., Previato, C., Addis, A., Zago, G., Kamsteeg, A., Dilaria, S., Canovaro, C., Artioli, G., Bonetto, J., 2019. Mineralogical clustering of the structural mortars from the Sarno Baths, Pompeii: A tool to interpret construction techniques and relative chronologies. Journal of Cultural Heritage 40, pp. 265-273 https://doi.org/10.1016/j.culher.2019.04.016

Secco, M., Dilaria, S., Bonetto, J., Addis, A., Tamburini, S., Preto, N., Ricci, G., Artioli, G., 2020. Technological transfers in the Mediterranean on the verge of Romanization: Insights from the waterproofing renders of Nora (Sardinia, Italy), Journal of Cultural Heritage, 44, pp. 63-82, https://doi.org/10.1016/j.culher.2020.01.010

Secco, M., Asscher, Y., Ricci, G., Tamburini, S., Preto, N., Sharvit, J., Artioli, G., 2022. Cementation processes of Roman pozzolanic binders from Caesarea Maritima (Israel). Construction and Building Materials 355, 129128 https://doi.org/10.1016/j.conbuildmat.2022.129128

Sekhaneh1, W. A., Shiyyab, A., Arinat, M., Gharaibeh, N., Use of FTIR and Thermogravimetric analysis of ancient mortar from church of the Cross in Gerasa (Jordan) for conservation purposes. Mediterranean Archaeology and Archaeometry 20, 3, pp. 159-174 http://dx.doi.org/10.5281/zenodo.4016073

Seymour, L. M., Keenan-Jones, D., Zanzi, G. L., Weaver, J. C., Masic, A., 2022. Reactive ceramic fragments from ancient water infrastructure serving Rome and Pompeii. Cell Reports Physical Science 3, 101024

Stepansky, Y. 2017. Tiberias. Israel Archaeological Survey.

Theodoridou, M., Ioannou, I., Philokyprou, M., 2013. New evidence of early use of artificial pozzolanic material in mortars. Journal of Archaeological Science 40, pp. 3263- 3269 http://dx.doi.org/10.1016/j.jas.2013.03.027

Vola, G., Gotti, E., Brandon, C., Oleson, J. P., Hohlfelder, R. L., 2011. Chemical, mineralogical and petrographic characterization of Roman ancient hydraulic concretes cores from Santa Liberata, Italy, and Caesarea Palestinae, Israel. Periodico di Mineralogia, 80, 2, pp. 317-338. DOI:10.2451/2011 PM0023

Weiner, S., 2010. Microarchaeology: Beyond the visible Archaeological record, New York.